Massachusetts Institute of Technology

Cambridge, Massachusetts 02139

TITLE

"Application of Gas Lasers to Studies of Fundamental Molecular and Atomic Processes"

Annual Technical Report # 2

for combined periods: January 1, 1969 to June 30, 1969
July 1, 1969 to December 31, 1969

Under Supervision of

Principal Investigator: Professor Ali Javan
617-864-6900 x5038

Under

Contract # N00014-67-A-0204-0014

Program Code # 8E30

Sponsored By

Advanced Research Projects Agency
ARPA Under No. 306

Contract Starting Date:	July 1, 1967
Contract Termination Date:	June 30, 1970
Contract Total:	$150,000
M.I.T. Project Number:	DSR 70620

Issued Date: April 10, 1970

Massachusetts Institute of Technology

Cambridge, Massachusetts 02139

TITLE

"Application of Gas Lasers to Studies of Fundamental Molecular and Atomic Processes"

Annual Technical Report # 2

for combined periods: January 1, 1969 to June 30, 1969
July 1, 1969 to December 31, 1969

Under Supervision of

Principal Investigator: Professor Ali Javan
617-864-6900 x5088

Under

Contract # N00014-67-A-0204-0014

Program Code # 8E30

Sponsored By

Advanced Research Projects Agency
ARPA Under No. 306

Contract Starting Date:	July 1, 1967
Contract Termination Date:	June 30, 1970
Contract Total:	$150,000
M. I. T. Project Number:	DSR 70620

Issued Date: April 10, 1970

CONTENTS

This progress report summarizes the ongoing research of the Massachusetts Institute of Technology Laser and Quantum Electronics Group, under ONR Contract #N00014-67-A-0204-0014, performed during the period January 1, 1969 to December 31, 1969. Research performed includes:

1. Generation of Short CO_2 Laser Pulses by Means of a Bistable Optical Element

Interest in obtaining short pulses from a CO_2 laser for use in studies of coherent interactions and relaxation in gaseous systems has led to the development of a bistable optical element which promises to be of general applicability in a wide variety of laser systems. The device consists of a Fabry-Perot cavity filled with a saturable absorber. When used as one mirror of a laser cavity, the device can be operated so as to switch rapidly from a high reflection, low transmission state to a low reflection, high transmission state and thus dump all of the energy stored in the laser cavity in a time comparable to the round trip time of the cavity. Other configurations are possible which permit repetitive Q-switching, stabilization of laser output intensity, conversion of CW laser output to an infinite pulse train of controllable separation and duration, and logical operations on two or more signals. Further details are given in Appendix I.

2. Rotational Relaxation Effects in CO_2 Observed in Standing Wave Saturation Resonances in Spontaneous Emission

(This work has been done jointly with Dr. Charles Freed of Lincoln Laboratories)

The rotational relaxation linewidth of CO_2 has been measured as a function of pressure by means of a standing wave saturation technique. In the experiment a low pressure CO_2 absorption cell at room temperature

is subjected to standing wave radiation from a single-mode CO_2 laser oscillating on a preselected 10.6μ P or R branch transition. The upper level of the transition belongs to the (001) vibrational state. The saturation effect is observed as a sharp decrease in spontaneous emission at 4.3μ [(001 → (000)] as the laser lines tuned through the center of the corresponding 10.6μ absorption line. At a low power level the width of the change signal is a measure of the relaxation rate in the (001) vibrational level. At higher powers, saturation broadening effects set in. Pressure shifts have also been measured.

The effect, which is closely related to the Lamb dip effect, may be understood as follows: The intense laser field produces an increase in the population of the (001) vibrational state. Because of rapid rotational relaxation this population increase occurs over a whole set of rotational levels. Accordingly, the 4.3μ fluorescence intensity increases over the entire band by an amount ΔI which is a nonlinear function of the laser field intensity. For a sufficiently intense laser field, ΔI decreases resonantly by a sizeable fraction as the laser frequency ν is tuned over a narrow frequency interval centered about the peak frequency of the Doppler profile, ν_0. The maximum of the resonance occurs at $\nu = \nu_0$ and its linewidth as a function of $\nu = \nu_0$ is determined by the CO_2 relaxation rate, the power broadening of the absorbing transition, are the broadening due to the molecular transit time across the diameter of the incident beam. This technique is applicable to other molecules, such as CO, and further experiments are planned.

3. Influence of Molecular Relaxation in Coherent Optical Processes

A series of relaxation studies is currently under way in which the fluorescence produced by short intense laser pulses passing through a resonant gaseous absorber is used to monitor the excitation density remaining after the pulse has traversed the medium. One may obtain considerable information on relaxation processes by studying the fluorescence intensity as a function of input pulse intensity ("fluorescence curve") under various conditions. The overall features of the fluorescence curve depend on the relative magnitudes of the pulse duration, τ_p, and the mean relaxation time, T, and on the input pulse field intensity (electric field of magnitude E). For sufficiently small values of the input field ($\Theta = \frac{\mu E}{\hbar} \tau_p \ll 1$, μ = transition matrix element), the excitation is proportional to Θ^2 and hence increases linearly with the pulse intensity. This statement remains true for $\frac{\mu E}{\hbar} \tau_p > 1$ provided $\frac{\mu E}{\hbar} T \ll 1$, except that in the latter case the slope of the fluorescence curve would be proportional to T^2 rather than τ_p^2. Note, however, that in any attempt to extract relaxation times from fluorescence measurements in the weak-field limit, one would also have to take into account the presence of non-radiative decay channels and radiation-trapping effects.

In the case of an inhomogeneously broadened line whose spectrum is wide compared to that of the excitation pulse, the initial E^2 dependence of the excitation goes over into a linear dependence upon E, i. e. becomes proportional to the square-root of the intensity, when the lesser of $\frac{\mu E}{\hbar} \tau_p$, $\frac{\mu E}{\hbar} T$ is ≈ 1. Therefore, given a knowledge of μ and the calibration of the intensity scale, it is possible to obtain the relaxation time from this transition region of the fluorescence curve.

An even more direct way to obtain this information would be to measure the fluorescence curve $\tau_p \ll T$ where, at appropriate values of field intensity (i.e., $\Theta = n\pi$), the self-induced transparency effect occurs. In this case, the sample is left in a completely unexcited state after the passage of the pulse. Accordingly, the fluorescence intensity from the upper level to some lower level is a minimum for this pulse, as compared with pulses of higher or lower energy. One thus expects to see maxima and minima corresponding to $\Theta = n\pi$ superimposed upon the background slope of the fluorescence curve. This effect provides both a calibration of the intensity scale and a direct measure of the relaxation time, since the presence of the maxima and minima is very sensitive to having $\tau_p < T$. The latter technique has the advantage that it can be used in dilute systems where the observation of self-induced transparency is impractical because of the small absorption coefficient. Furthermore, calculations show that the effect should be observable, although smaller, in degenerate systems.

Experiments are currently in progress to observe these effects in the 4.3μ ($00^0 1 \rightarrow 00^0 0$) fluorescence of CO_2 excited by a 10.6μ CO_2 laser. Initial observations show the transition from the quadratic to the linear dependence on E. As expected, this transition region shifts to lower power levels as the CO_2 pressure is lowered. At very low pressures, some indication of the presence of flattened regions in the excitation curve are noted, but no dips of the magnitude expected have been observed yet. Computer calculations using realistic pulse shapes and including relaxation effects are being made and some of these, together with experimental results, are shown in Fig. 1. Work is also proceeding on obtaining laser pulses with better amplitude and frequency stability as well as spatial uniformity -- characteristics which are essential for observing the maxima and minima in the fluorescence curve.

4. Propagation of Intense Short Pulses Through SF_6

Experimental studies of the propagation of short pulses of 10.6μ CO_2 laser radiation through an SF_6 absorber as a function of absorber pressure and of incident pulse intensity, have been completed together with a detailed theoretical explanation of the observations.

It has been shown both experimentally and theoretically that pulse reshaping and pulse delays can be obtained in systems with degenerate energy levels even under conditions which preclude self-induced transparency. The pressure and intensity regimes for which this is true in SF_6 have been elucidated. Complications due to apparent self-focusing effects at high pressure and high intensity have been noted. (See Appendix II for further details.)

A theoretical treatment has also been given of the propagation of "Zero π" pulses through degenerate media. Such pulses result if one introduces a 180° phase change between the leading and trailing halves of a pulse in such a way that $\int_{-\infty}^{\infty} E dt = 0$. For coherent excitation, the effect of the second half of the pulse is essentially to undo the action of the first half of the pulse, and this is true independent of the matrix element of the transition. The propagation of these pulses is therefore not qualitatively altered by level degeneracy, as is the case for the propagation of 2π pulses. In the absence of relaxation, zero degree pulses are expected to propagate with relatively little loss of energy but considerable distortion, and would be a much more sensitive indicator of relaxation processes than 2π pulses in degenerate media, where the coherent interaction effects are masked by the degeneracy.

5. Study of the CO Laser and Plans for the Investigation of Chemical Lasers in the Near Infrared

Plans are under way for a detailed examination of the excitation and relaxation processes occurring in the efficient CO laser. These include attempts towards observing laser oscillations on the vibrational overtones corresponding to the $v \rightarrow v-2$ transitions, which fall in the 2.5μ region. The investigation may possibly be extended to chemical lasers such as HF and DF. One goal is to obtain oscillations on vibrational overtones in these molecules by inhibiting the $v \rightarrow v-1$ oscillations. This would open the possibility of obtaining efficient laser oscillations in the 1 to 1.5μ region. The above studies are being planned simultaneously with an investigation of detailed relaxation mechanisms.

APPENDIX I

A BI-STABLE OPTICAL ELEMENT AND ITS APPLICATIONS

A. Szöke, V. Daneu, J. Goldhar, and N.A. Kurnit
Department of Physics, MIT, Cambridge, Mass. 02139

In this publication we describe the operating principles and our first experiments on an optical element which has two stable states in a certain range of input intensities. The basic element is a resonant optical cavity filled with a saturable absorber (a "saturable resonator"). It is passive in the sense that its only energy source is provided by the incident light beam itself. First the operating principles are described, then some applications to produce short and strong light pulses are given. An arrangement is described which can produce pulses of variable length and intensity and also infinite optical pulse trains when excited by a continuous wave laser. Finally, we remark on switching characteristics.

Bi-stable and non linear optical devices using lasers, whose oscillation is stopped by other lasers were described earlier[1]. These used gain and saturable absorbing elements in the same cavity. It will be shown below that in the presence of an external light beam incident on a cavity a saturable absorber alone can give these characteristics. As a consequence many types of lasers can be used; the device becomes more flexible and has a large range of applications.

Consider a Fabry-Perot resonator filled with a saturable absorber. We assume that a plane monochromatic light wave impinges on the resonator, and that when the absorber in the cavity is bleached, the cavity is adjusted to exact resonance. To simplify our discussion, we consider steady state only, and we also assume that exact resonance is maintained even when the absorber is not saturated. The mirrors are characterized by their electric field transmission and reflection coefficients, τ and ρ respectively. For complex fields these are complex numbers, which for negligible mirror loss satisfy $1 = \tau - \rho$, $1 = |\rho|^2 + |\tau|^2 = R + T$, where R and T are the usual reflectivity and transmissivity of the mirror. The cavity equations for the fields at mirror 1 at some time t are

$$E_2' = \rho E_2 e^{-2 i k \ell - \alpha \ell}$$

$$E_2 = \tau E_1 + \rho E_2' ; \qquad (1)$$

subscripts are defined in Fig. 1. The absorption coefficient of the material, α is defined as usual. The solution of these equations exhibits the Fabry-Perot

resonance,

$$E_2 = \tau E_1 \left[1 - \rho^2 e^{-2 i k \ell} e^{-\alpha \ell} \right]^{-1} . \qquad (2)$$

The transmitted and reflected power can then be calculated from the equations

$$E_3 = \tau E_2 e^{-i k \ell} e^{-\alpha \ell / 2} ,$$

$$E_1' = \rho E_1 + \tau E_2' . \qquad (3)$$

In a saturable absorber, α is a decreasing function of the local intensity $I_2 = (c/8\pi) |E_2|^2$. The crux of our argument is that for a range of input intensities, I_1, Eq. (2) can have two solutions. In one of them, the resonance is prevented by the absorber, most of the energy is reflected, and the field penetrates but little into the cavity. There are not enough photons to saturate the absorber; if the absorption is strong, $I_2 \approx I_1 T$ and $I_1' \approx I_1 R$. In the other state the absorber is bleached; the intensity inside the resonator is enhanced to a value of $I_2 \approx I_1 / T$, and in this ideal case all the light is transmitted. There is little reflection and all the light is "available" to bleach the absorber.

We proceed now to present a more detailed though oversimplified solution for a simple two-level absorber and a resonator with high reflectivity mirrors, $T = 1 - R << 1$. For high reflectivity mirrors, little absorption is needed to spoil the resonance: in particular, the strength of the resonance is determined by the dimensionless parameter $k = R \alpha \ell / (1 - R)$. Thus, there is a range of absorption coefficients such that $\alpha \ell << 1$, but $k >> 1$. These conditions are overly restrictive, but they allow simplification of the above equations which then yield (on resonance):

$$I_2 = \frac{I_1}{T} \frac{1}{(1 + k)^2} \qquad (4a)$$

$$I_1' = \frac{I_1}{R} \left(\frac{k}{1 + k} \right)^2 \qquad (4b)$$

$$I_3 = I_1 \frac{1}{(1+k)^2} . \qquad (4c)$$

Our absorber model is a simple two-level system with a single relaxation time τ_R. It obeys the rate equation

$$\frac{dn_u}{dt} = \frac{\alpha I_2}{\hbar\omega} - \frac{n_u}{\tau_R} \qquad (5)$$

where n_u is the no. of molecules in the upper (excited) state, α is the intensity-dependent absorption coefficient, and $I_2/\hbar\omega$ is the incident photon flux. The absorption coefficient α satisfies the equation of stimulated emission,

$$\alpha / \alpha_0 = (n_\ell - n_u)/N, \qquad (6)$$

where $n_\ell = N - n_u$. N is the total number of molecules per cm^3 and α_0 is the low light level absorption coefficient. In steady state Eqs. (5) and (6) give

$$\alpha = \alpha_0 (1 + I_2/I_0)^{-1},$$
$$I_0 = \frac{\hbar\omega}{2\tau_R}\left(\frac{N}{\alpha_0}\right) . \qquad (7)$$

The threshold intensity I_0 depends on the ratio of the relaxation rate $1/\tau_R$ to the mean molecular absorption cross section α_0/N. Substitution of Eq. (7) into (4a) shows that $I_1/(I_0 T) = z_1$ can be expressed as a single-valued function of $I_2/I_0 = z_2$:

$$z_1 = z_2 \left(1 + \frac{k_0}{1+z_2}\right)^2 \qquad (8)$$

The general behavior of this function is sketched in Fig. (2a). For high values of z_2 the slope $z_1/z_2 = 1$; this is the resonance condition. For low values of z_2 we get the slope of the resonance in the presence of absorption $z_1/z_2 = (1 + k_0)^2$. Calculation of the derivative shows that for values $k_0 > 8$ there is a maximum and a minimum on the curve. We can then predict for $k_0 > 8$, that if I_1 is slowly increased when a point of maximum of the curve of Fig. (2a)

is reached, the resonator will switch over discontinuously from a "low intensity-high absorption" to a "high intensity-low absorption" state. If a point of minimum is reached, coming from the high intensity side, a reverse transition occurs. Thus, a bistable optical element is obtained, exhibiting hysteresis. It can be shown that the steady state solutions are stable with respect to infinitesimal perturbations.

In the more general case, where 1 - R is not small enough to warrant the above approximations, the curves can be plotted with the aid of a digital computer, using the more correct form of Eqs. (1) - (3) where $\exp [- \alpha \ell]$ is always replaced by $\exp [- \int_0^{\ell} \alpha (z)\, dz]$. The absorption coefficient $\alpha (z)$ is still given by Eq. (7) using $I_2 (z) = I_2 (0) \exp [- \int_0^{z} \alpha (z')\, dz']$. One such plot is given in Fig. (2b) for $1 - R = 0.2$. Note the similarity of the curves in Fig. (2) to the pressure vs. density isotherms of a gas-liquid phase transition with a critical point.

Our calculations are still oversimplified since we do not take into account the standing-wave nature of light that will bleach the absorber in the form of a grating and the variation of light intensity across the beam. Also, real life saturable absorbers are not two level systems; in particular they may have a large residual absorption.

A time-dependent version of Eq. (1) can be easily obtained. If the input field is suddenly switched on, the field inside the cavity rises exponentially:

$$E_2 (t) = (E_1 / \tau) [1 - \exp - (t / t_r)]$$

the risetime being $t_r = (2\ell / c) (1 - R)^{-1}$. Examination of the equations with the absorber present shows that the risetime is even shorter. A saturable resonator of .1 cm thickness and 95% reflectivity has a switching time of $\sim 10^{-10}$ seconds. In a gaseous saturable absorber, if the length of the pulse is longer than the inverse Doppler width, this risetime is lengthened to the inverse Doppler width: this is the time it takes for two unsaturated molecules to move through one wavelength and thus be saturated by the standing wave field.

Our first experiments demonstrate the above characteristics. We put a saturable resonator in the output beam of a single Q-switched frequency, single axial mode CO_2 laser [2], [3] on the P(16) 10.6 μ transition. The resonator is 2 cm long, and it has BaF_2 mirrors coated with a single $\lambda/4$ layer of Te. The mirrors are flat to better than 1/5 red (6328 Å) fringe. The resonator is tuned by heating its spacers to a stabilized temperature. It is connected to a vacuum pump, and it can be filled to various pressures of SF_6 gas, a strong absorber of this transition.[4] Fig. (3) shows clearly the nonlinearity obtained this way, although the pressure of the absorber was not high enough to bring us to the bistable region.

The saturable resonator was used in a cavity-dumping device. This device (at least in its ideal form) accomplishes the same essential function as those described by Bridges and Cheo[5] and others[6] without the use of an external modulator. As illustrated in Fig. (4a), we replace one of the laser mirrors by a saturable cavity. Q-switching or mode-locking is initiated in the usual way. (In our experiment, we used a rotating mirror.) If the saturable cavity operates in its bistable region, if its switching time is short, and if the cavity is tuned to resonance, we expect a sudden increase in the transmission of the cavity at the appropriate intensity of the laser. Thus in the ideal case of 100% transmission of the saturable resonator, a pulse is obtained whose physical length is twice the length of the laser. It should be emphasized that in the high absorption region the laser light does not "see" the third mirror, thus alignment of the laser is not critical. Experimental results are presented in Fig. (4b), (c). Fig. (4b) shows the laser output with an off-resonance, empty Fabry-Perot. The upper trace is the output of the cavity through the single mirror; the lower one is the output through the resonator. The difference in the shape and timing of the pulses is instrumental. The oscilloscope is triggered externally so any change in the relative position of the pulses is signifi-

cant. Fig. (4c) shows a picture similar to (4b) with the saturable resonator adjusted to resonance and filled to 1.5 torr SF_6 ($\alpha_0 \ell \sim 2.5 - 3.5$). A 50 nsec wide pulse of ~ 100 watt peak power comes out through the saturable resonator (the laser round trip time, $2 L/c = 35$ nsec). At the same time, the output on the other end of the cavity drops. This experiment clearly demonstrates the working principles of the device. Switching levels at which cavity dumping occurs can be designed at will using the length of the cavity - affecting principally k_0 - and the relaxation time τ_c which, in the case of gaseous absorbers (SF_6), can be affected by the addition of a buffer gas (He).

The rest of this letter presents some other interesting applications of saturable cavities. They all operate on paper; we also demonstrated some of them in the laboratory. 1.) In the configuration of Fig. (4a), the resonator can be operated outside the bistable region, either by low absorption ($k_0 < 8$) or by choosing the laser intensity too high. In this region, if the time behavior does not become unstable, we expect to stabilize the laser output intensity and thus also operate it in a single mode: if the laser intensity grows, the dye bleaches and the output increases, thus decreasing the round-trip gain of the laser.[6] 2.) In the same configuration of Fig. (4a), the saturable cavity can be detuned from exact resonance; in the high absorption region region the reflectivity is essentially $R_A = 1 - T$, while if the absorber is bleached, the reflectivity changes to $R_B = 1 - T^2$. Thus, an increasing laser intensity leads to an increasing loop gain and the laser performs repetitive Q-switching at intervals determined by the pumping rate. This behavior was seen by us experimentally[7]. 3.) The arrangement shown in Fig. (5), if designed properly, produces an infinite pulse train from a constant (CW) light input; it behaves like a monostable multivibrator. The saturable cavity (mirrors 2, 3) has to operate in the bistable region. The light intensity in the empty cavity (mirrors 1, 2) grows, then it switches out and the cycle repeats. The pulse duration is $2L/c$, and

the time between pulses is determined by the input intensity, the Q of the empty cavity, and the switching level. The time between pulses cannot be longer than the cavity holding time, Q (2L/c). If the same arrangement is fed by a pulsed (Q-switched) laser of appropriate duration, a single pulse of duration 2L/c can be obtained. For a ruby laser input pulses of 10-1000 psec range can be realized. 4.) A saturable cavity can be brought from one state to another (e. g., to high transmission) by shining light on it from an external source (e. g., another laser). Such an arrangement performs a basic logical operation on two signals. Furthermore, if the hysteresis is large enough, once switched over to a high transmission state, the device will stay in that state as long as the input is maintained, thus performing a basic memory operation. Particularly interesting is the case where the two input beams are both parallel to the resonator axis; we know from the mode structure of cavities that an incident light beam of width $r = (\ell \lambda)^{1/2}$, where ℓ is the length of the cavity and λ the wavelength, interacts weakly with a similar beam parallel to it at a distance comparable to r. Consequently, many adding and memory operations can be performed in parallel.

ACKNOWLEDGEMENTS

The authors wish to thank Prof. A. Javan and Dr. F. Zernike for fruitful discussions.

REFERENCES

(1) G.J. Lasher and A.B. Fowler: IBM J. Res. Develop. 8, 471 (1964); G.J. Lasher: Solid-state Electron. 7, 707 (1964); C.J. Koester, R.F. Woodcock E. Suitzer, and H.M. Teager: J. Opt. Soc. Am. 52, 1323 (1962); A.B. Fowler: Appl. Phys. Letters 3, 1 (1963). Chapters 16 and 17 in Optical and Electro-Optical Information Processing, edited by James T. Tippet, David A. Berkowitz, Lewis C. Clapp, Charles J. Koester, and Alexander Vanderburgh, Jr., M.I.T. Press, 1965. Yu. P. Zakharov, V.V. Nikitin, V.D. Samoilov, A.V. Uspenskii, A.A. Sheronov, Sov. Phys. Semiconductors 2, 623 (1968).

(2) The laser is of standard design, uses a flowing CO_2 - N_2 - He mixture; it is Q switched $\sim$ 50/sec by a rotating mirror. The frequency selective element is either a grating of 75 lines/mm. or alternatively a low order, off axis Fabry-Perot resonator.(3) For a more detailed desc ription of the apparatus, see also Ref. (4)

(3) V. Daneu, Appl. Optics, 8, 1745 (1969)

(4) C.K. Rhodes, A. Szöke, Phys. Rev., (to be published August 5 issue).

(5) T.J. Bridges and P.K. Cheo, Appl. Phys. Letters 14, 262 (1969).

(6) A.A. Vuylsteke, J. Appl. Phys. 34, 1615 (1963); W.R. Hook, R.P. Hilberg, and R.H. Dishington, Proc. IEEE 54, 1954 (1966); see also review by A.J. DeMaria, D.A. Stetser, and W.H. Glenn, Jr., Science 156, 1557 (1967).

(7) Points (2), (3) above were realized four years ago by V. Daneu, G. Soncini, and O. Svelto at the Instituto di Fisica del Politecnico in Milan, who performed experiments on the stabilization of ruby lasers; V. Daneu, private communication.

FIGURE CAPTIONS

Fig. 1: Schematic diagram of a Fabry-Perot resonator. The electric fields are defined on the mirrors 1 and 2. Arrows show direction of propagation.

Fig. 2: Static characteristics of a Fabry-Perot resonator filled with a saturable absorber. (a) From Eqs. (4), and (b) from computer calculation.

Fig. 3: Multiple oscilloscope photograph of Q-switched pulses from a CO_2 laser operating on the P (16) 10.6 μ line after light has passed through 2 cm long Fabry-Perot resonator tuned to resonance. The two traces show the output pulse from an empty cavity with ~ 70% transmission, and from a cavity filled with 1 torr SF_6. Note the cutoff of the tail end of the pulse in the latter.

Fig. 4: "Passive" cavity dumping device. (a) Experimental arrangement (b) and (c) laser output: upper trace, output through single mirror; lower trace, output through resonator. (b) resonator empty, off resonance. (c) resonator on resonance, filled with saturable absorber. Output through resonator ~ 100 watt.

Fig. 5: Double-cavity arrangement to produce light pulses of duration 2 L/c. The saturable cavity (mirrors 2, 3) operates in the bistable region.

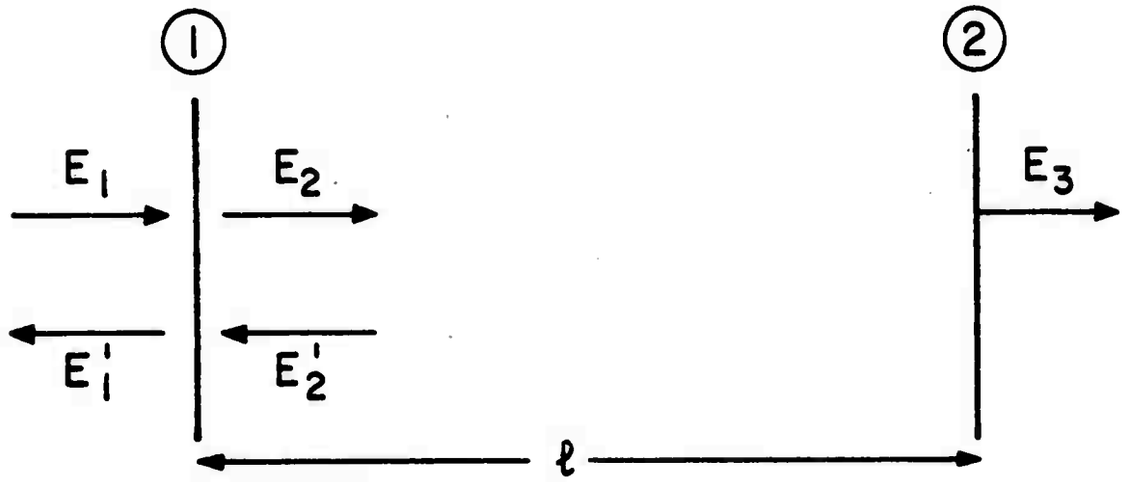
1
2
E1
E2
E3
E1'
E2'
ℓ

FIG. 2

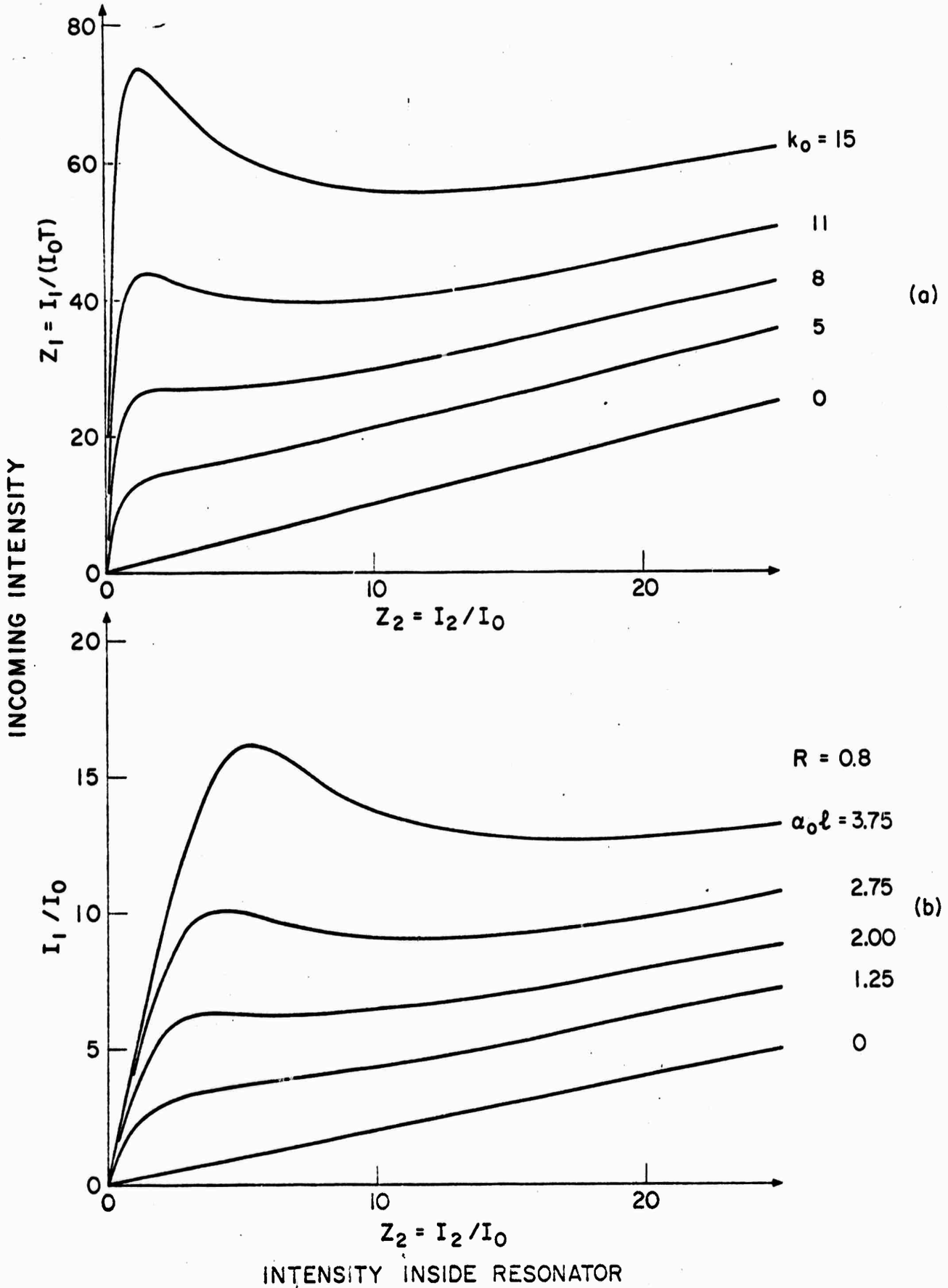
80
60
40
20
0
$Z_1 = I_1/(I_0T)$
$k_0 = 15$
11
8
5
0
(a)
0
10
20
$Z_2 = I_2/I_0$
INCOMING INTENSITY
20
15
10
5
0
I_1/I_0
R = 0.8
$\alpha_0 \ell = 3.75$
2.75
2.00
1.25
0
(b)
0
10
20
$Z_2 = I_2/I_0$
INTENSITY INSIDE RESONATOR

FIG. 3

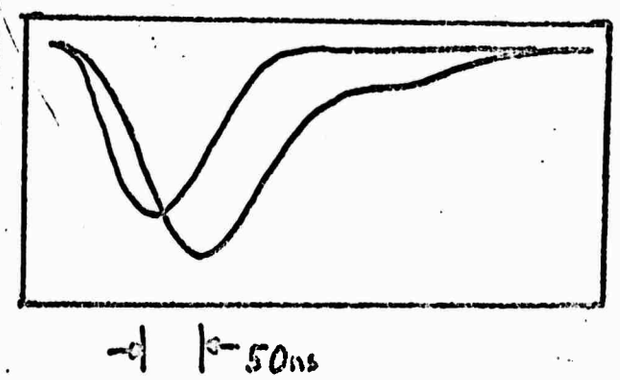

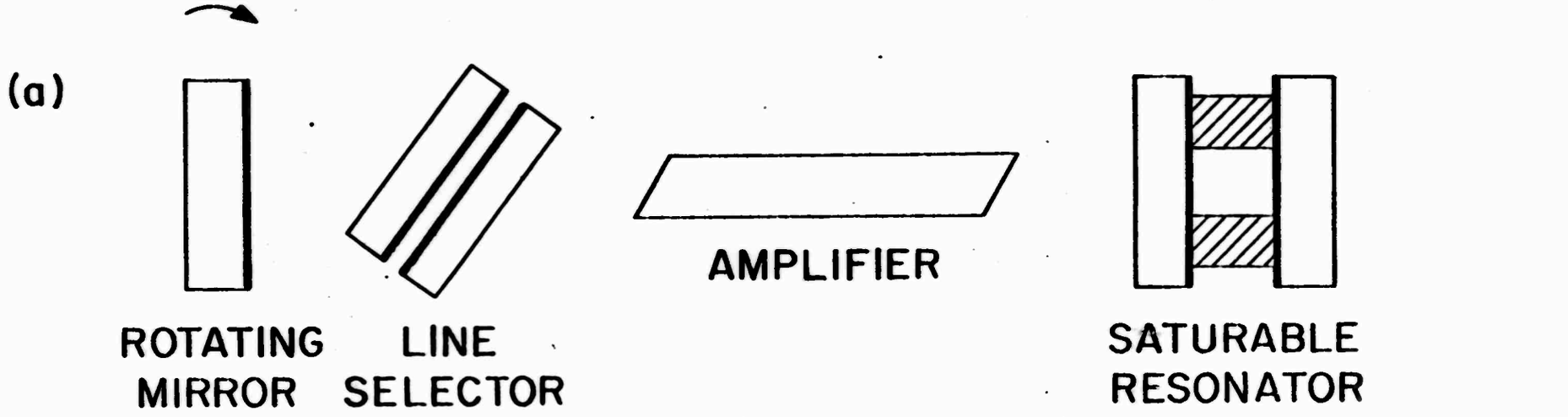
(a)
ROTATING MIRROR
LINE SELECTOR
AMPLIFIER
SATURABLE RESONATOR

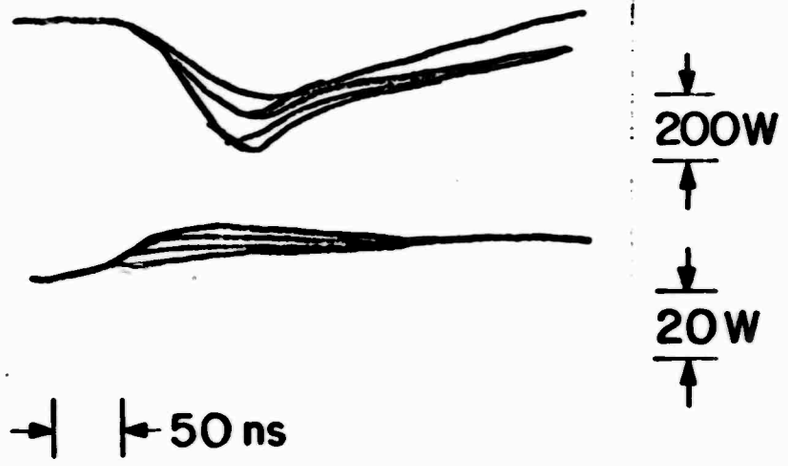
200W
20W
50 ns

(b)

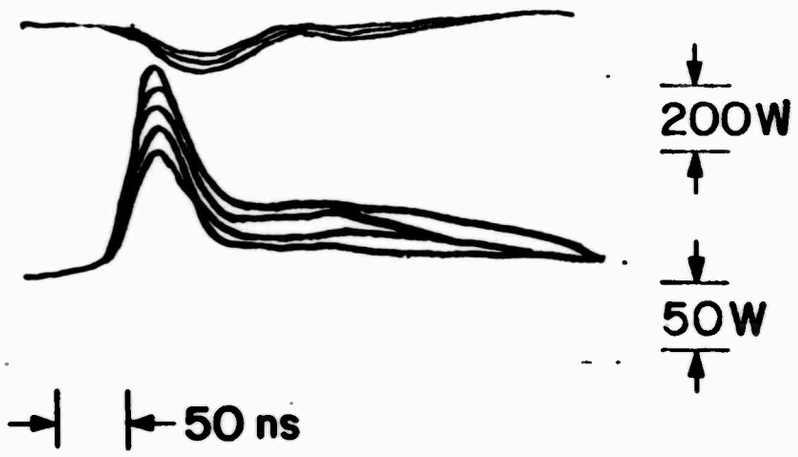
200W
50W
50 ns

(c)

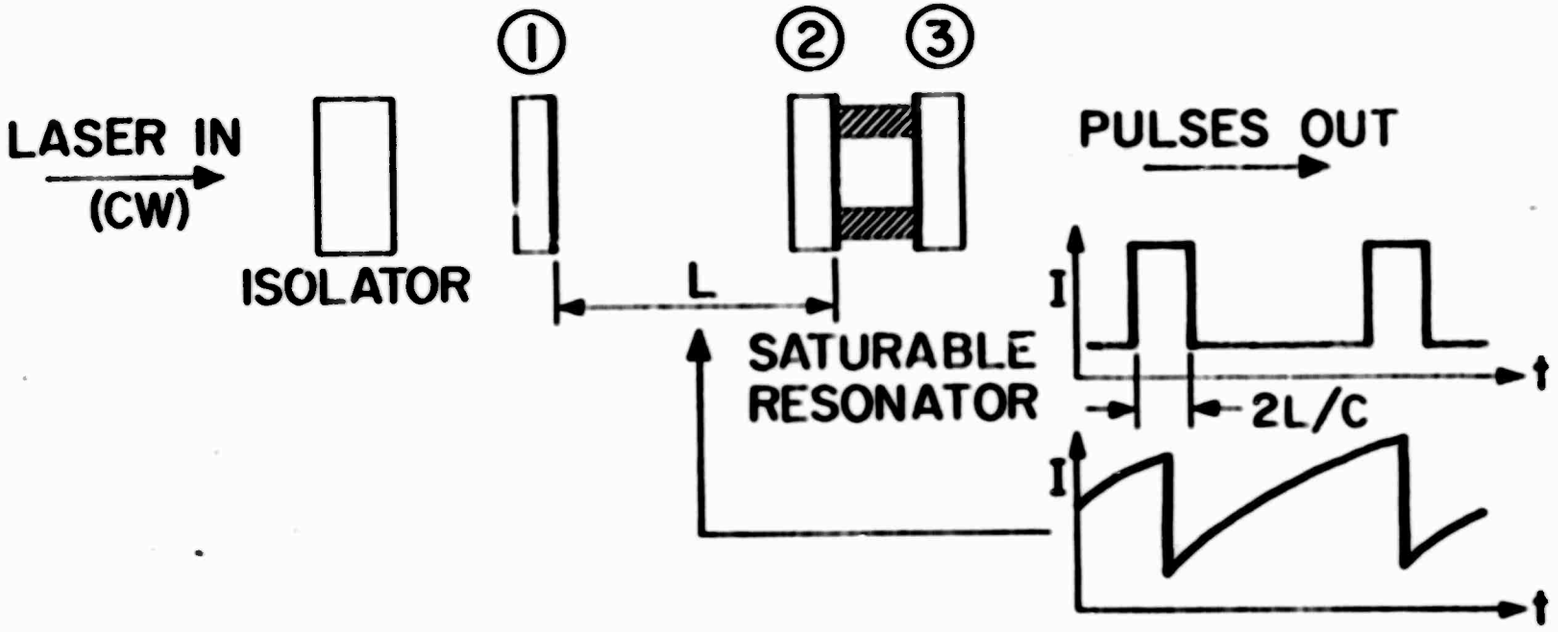
LASER IN
(CW)
ISOLATOR
①
②
③
L
SATURABLE
RESONATOR
PULSES OUT
I
2L/C
I

APPENDIX II

TRANSMISSION OF COHERENT OPTICAL PULSES IN GASEOUS SF_6

C. K. Rhodes and A. Szöke
Physics Department, MIT, Cambridge, Mass. 02139

I. Introduction

A number of results, both experimental and theoretical, have been obtained on the behavior of optical pulse propagation through an absorbing medium. The experiment involved a Q-switched CO_2 laser as the source; the absorbing medium was gaseous SF_6. We also present some experimental results on the spectroscopy of SF_6 which bear on the pulse transmission experiments. On the theoretical side, we present some analytical results based upon a simplified model discussed previously.[1] That model neglects inhomogeneous broadening; in the degenerate case its use is entirely justified. The calculations are substantiated by some considerably more detailed computer results.[2] Both calculations corroborate the experimental findings.

This article emphasizes the influence of level degeneracy (whether spatial or otherwise) on the propagation of coherent radiation. These considerations arise in a natural way in connection with the problems of self induced transparency[1, 3, 4] and photon echo.[5, 6]

The article concludes with three appendices. The first presents some unusual observations of pulse reshaping in SF_6. The experimental evidence appears to indicate the presence of a focusing effect.[3] The second appendix gives the results of calculations relevant to an experiment on CO_2, similar to the transient nutation well known in N.M.R, that would enable the measurement of the dephasing time T_2. This experiment does not involve a propagation effect. The third contains some remarks on the polarization dependence of the photon echo[5, 6] and the modifications that arise for an optically thick sample.

This article is divided into the following sections.

II. Experimental Apparatus

A schematic of the experimental apparatus is illustrated in Fig. (1). The cavity of the CO_2 laser is bounded by the grating G and the curved Ge mirror M. Q-switching is accomplished by the rotating mirror R. Adjustment of the grating G enabled operation on a single vibrational-rotational transition in the 10.6μ band. The wavelengths were determined by direct measurement with the monochromator K, previously calibrated with a 6328Å He-Ne laser and corrected to the vacuum. The identification of the particular transitions used in this experiment was unambiguous. A typical output pulse is shown in Fig. (2). Its width is given by $\tau \cong 300$ nsec. The temporal coherence of the pulses was determined by direct examination of the signal modulation generated by beating the Q-switched pulse against an independent continuous wave CO_2 laser in a Au:Ge detector. Since the two lasers were operating independently, the variation of the beat note frequency during the Q-switched pulse establishes an upper bound on the change of the optical carrier frequency which occurs during the Q-switching process. If $\Delta\omega$ represents the total change in optical frequency during the Q-switched pulse, it was found that $\Delta\omega \lesssim 2\pi/\tau$; hence, enabling one to validly represent the pulse in the form $E(t) = \mathcal{E}(t)\cos\omega t$, with slowly varying $\mathcal{E}(t)$. The pulse intensity was varied by an adjustable, linear attenuator. This was accomplished by filling cell S_1 with an appropriate amount of methyl ether (pressure = 1 - 100 Torr). The linearity of this attenuator is assured by operating at a pressure sufficiently high so that all relaxation rates are $>> 1/\tau$. A fraction of the input pulse was passed through the monochromator K and detected at detector D_1. The remainder was directed through a 3.4 meter SF_6

absorption cell in which the SF_6 pressure could be reliably set to any pressure from 1 mTorr to 10 Torr. This SF_6 pressure was measured by a McLeod gauge. The output pulse was detected at D_2, amplified (if necessary) and photographed directly on the CRT of a Tektronix 585 oscilloscope. The detector D_3 sensed the Q-switched signal which was reflected from the grating zero. This pulse established a trigger signal independent of the intensity of the pulse passing through the cell S_2. Two types of pulse measurements were made. One involved the recording of the signal at D_2 for a fixed SF_6 pressure in cell S_2 while the input pulse intensity was changed by varying the methyl ether pressure in cell S_1. The other corresponded to constant input pulse intensity while the SF_6 pressure in cell S_2 was slowly changed.

The CO_2 laser is of standard design with NaCl Brewster windows and a flowing CO_2-N_2-He gas mixture. Detectors D_1 and D_3 were Ge:Au operated at 77°K while detector D_2 was Ge:Cu operating at liquid helium temperature. The system rise time (detector and electronics) for detector D_2 was less that 8 nanoseconds as determined by direct measurement.[7]

III. Experimental Results

A. SF_6 Spectroscopic Data

A series of experiments was performed with the object of determining the relative absorption and absorption versus pressure behavior of various CO_2 laser oscillations in gaseous SF_6. Figure (3) shows the linear absorption data corresponding to the P(16), P(18) and P(20) CO_2 lines for SF_6 pressures under 50 mTorr. These measurements were made with the apparatus illustrated in Fig. (1) but with the rotating mirror R replaced by a stationary one to permit continuous wave operation, and detector D_2

followed by a lock-in amplifier system. Input signal intensity was ~ 1mWatt. Significant attenuation occurs on all three lines with the P(16) line experiencing the greatest absorption. Since the Doppler width at 10.6μ for SF_6 is 30 MHz, these lines should be essentially inhomogeneously broadened for the SF_6 pressures less than 50μ mTorr. It should be noted that previous work[6] reports observations that are contrary to those shown in Fig. (3). They[6] describe the absorption as appreciable on only <u>one</u> line for SF_6 pressures below 1 mm Hg and identify this as the P(20) line of CO_2.

The behavior of coherent excitations is strongly influenced by the precise nature of the states involved. As an example, a simple model describing the effect of spatial degeneracy has previously been described.[1] In the case of SF_6, it is not obvious a priori that the transitions in the 10.6μ band are resolved with respect to their Doppler widths. Indeed, in the region of a Q-branch there is considerable likelihood that this is not the case. For definiteness let us consider the absorption of the P(16) line of CO_2. If this were caused by a single well resolved transition, then one would expect the absorption to initially increase linearly with pressure and then become, at sufficiently high pressure, pressure independent when the transition is fully pressure broadened. At even higher pressure neighboring lines overlap and the absorption rises again. Experimentally, no such pressure independent region is observed. On the contrary, the absorption exhibits no inflection points and rises linearly all the way from zero to 17 mm Hg which is well above any reasonable limit for pressure broadening. We believe that this constitutes unequivocal evidence against the hypothesis which states that the strong absorption of P(16) is due to a single well resolved resonance in SF_6. Similar behavior was also recorded for the P(18) CO_2 line. This is an unfortunate complication,

but a crucial one in the understanding of self-induced transparency and photon echo experiments in SF_6.

From a spectroscopic point of view our findings can be summarized as follows. The P(16) line of CO_2 exhibits the maximum absorption in SF_6 although the P(18) and P(20) lines are also appreciable absorbed. The transitions involved in these absorptions of P(16) and P(18) are not well resolved in relation to their Doppler widths. Figure (4), taken from Brunet[8] shows the 10.6μ band of SF_6 and the relative positions of the CO_2 lines according to McCubbin.[9] It is significant that the absorption of the laser radiation is in rough agreement with the low resolution spectrum obtained by Brunet.[8] This strongly suggests that the band has many overlapping transitions and behaves like a continuum absorber. Indeed, in a later section, a continuum model will be introduced in the description of the behavior of SF_6.

B. Pulse Experiments Conducted at Low Radiation Intensity and Low SF_6 Pressure (~10 mTorr)

In order to examine carefully the transition from the linear absorption region to the nonlinear region we worked at greatly reduced intensities for these runs ($\sim 10^{-3}$ of available intensity). We also operated at low pressures (~10 mTorr SF_6) so that the inequality $T_2 >> \tau = 300$ nsec would be beyond suspicion. In particular we were concerned with the time delay of pulses in this nonlinear transition region together with the relative intensities of the transmitted radiation. It should be pointed out that the electronics were all triggered by detector D_3 which was independent of the intensities of the incident and transmitted pulses. Thus the relative positions of the photographed pulses with respect to one another are real, not artificial. Three CO_2 transitions were examined in detail, P(16), P(18) and P(20). Figure (5) illustrates a sequence

of output pulses, at constant SF_6 pressure, for varying input amplitude of the P(16) lines. The first pulse in the sequence was nearly the minimum detectable intensity; its shape is that of the input pulse and its delay is observed to be very small. As the input intensity is raised, the delay is observed to increase while the pulse reshapes dramatically. As the input intensity is raised further, the delay of the pulse peak is reduced and the pulse assumes the shape corresponding to the input pulse. Figure (6) illustrates the relative time position of the output pulse peak as a function of output intensity for the P(16) transition. It is significant to notice that the reversal of the delay curve, Fig. (6), occurs at an intensity which corresponds to the knee of the saturation curve, Fig. (7). Some recent calculations by Hopf and Scully[10] indicate such effects. Similar behavior was noted on both the P(18) and P(20) transitions. However, in these cases the results are not as prominent since the P(18) and P(20) lines are absorbed less strongly than the P(16). However, a central point remains; the behaviors of all three transitions P(16), P(18), and P(20) were qualitatively similar.

The sequence of photographs in Fig. (5) shows that the pulses possess a sharp peak at the leading edge corresponding to the sharp peak at the front of the input pulse. This small peak has precursor type behavior. The saturation curve for this peak drawn in Fig. (7) shows that it is transmitted linearly as a function of input intensity in contrast to the remainder of the pulse.

C. Pulse Experiments Conducted at High Radiation Intensity and Moderate SF_6 Pressure (~40 mTorr)

An interesting effect was observed at high input intensities (i.e. intensities well above the knee on the saturation curve shown in Fig. (7). In

this experiment the input intensity was held constant while the pressure in the SF_6 cell was continuously lowered at a slow pumping rate. Figure (8) shows a sequence of photographs taken during one such run for the P(16) transition of CO_2. The largest pulse corresponds to an empty cell and thus is really the input pulse itself. The other pulses are at progressively higher pressure, in the obvious order. The photograph clearly shows a reshaping of the leading edge at an intermediate SF_6 pressure around $40 \sim 50$ mTorr. This steepening corresponds to a rise time of 30 nsec. Care must be taken to have a properly loaded detector as ringing can occur which will distort the pulse shape. This steepening can occur from a trivial population saturation effect, but as we will show, the behavior also occurs in a system with many overlapping levels even with a fully coherent excitation. This will be called an effective population saturation effect and as in the simple incoherent population saturation effect it corresponds to an energy loss from the propagating pulse. Machine calculations[2] have been made which exhibit this sharpening effect in the limit of coherent excitation, $T_2 > \tau_{pulse}$. The computations will be described in a later section of this paper. The effect was seen appreciably only on the P(16) line of CO_2; probably on the P(18) and P(20) lines there were not enough absorption lengths in the sample tube.

IV. Theory and Calculations

A. Calculations Corresponding to the Conditions of Section III B

In this section we present a simple model to account for the results obtained at low SF_6 pressure (~ 6 mTorr) and relatively low excitation (i.e. in the region of the knee of the saturation curve Fig. 7). Since the absorption

measurements described in section III A strongly suggest that a number of overlapping transitions are involved in the absorption of the CO_2 P(16) transition, we introduce a continuous distribution of dipole moments $n(\mu)$. The quantity $n(\mu)\,d\mu$ equals the density of systems possessing dipole moments between μ and $\mu + d\mu$. That is, we approximate the true physical situation with an effective continuum of dipole moments. The extent to which this assumption is valid depends upon the nature and density of the overlapping levels. We simply remark that this is not unreasonable, since the Q-branch electric dipole matrix elements for a symmetric top are proportional to the product $mk/[j(j+1)]$ for linearly polarized radiation, where $-j \leq m \leq j$ and $-j \leq k \leq j$, with m and k integral. This dependence, for sufficiently high j, will produce a large distribution of matrix elements, particularly, if several overlapping transitions are involved in the absorption.

The basic properties of such a model are illustrated with the choice of $n(\mu) = n_o$ (a constant) for $-\mu_m \leq \mu \leq \mu_m$ and $n(\mu) = 0$ otherwise. As further approximation, it is assumed that all the systems are on exact resonance, $\omega = \omega_o$; any inhomogeneous broadening is ignored and the pulse length τ is regarded as much less than the inverse of the homogeneous line width, T_2. These conditions are precisely those presumed in Ref. (1). We define

$$\Theta(\mu) \equiv \frac{\mu}{\hbar} \int_{-\infty}^{\infty} \mathcal{E}(t)\,dt \equiv \mu\phi \qquad (1)$$

where

$\mathcal{E}(t)$ = optical electric field amplitude

and

τ = pulse width $\ll$ dephasing time T_2.

Then, in analogy with Ref. (1), the polarization density $P(\phi)$ of the medium after the pulse has passed[11] is given by

$$P(\phi) = N \sum_{\{\mu\}} \mu \sin \Theta(\mu) \Rightarrow \int_{-\mu_m}^{\mu_m} n(\mu)\, \mu \sin \Theta(\mu)\, d\mu \qquad (2)$$

where N describes the density of systems and the sum is converted to an integral because the distribution $n(\mu)$ is continuous (cf. Ref. (1), formulae 5, 7, and 8). The evaluation of the integral in expression (2) yields

$$P(\phi) = 2 n_o \mu_m^2 j_1(\mu_m \phi) \qquad (3)$$

where $j_1(x)$ is the spherical Bessel function of the first kind of order one. For comparison, the polarization density $P_1(\phi)$ for a simple non-degenerate two-level system with matrix element μ_o is written

$$P_1(\phi) = N \mu_o \sin(\mu_o \phi) \qquad (4)$$

where N designates the density of atomic systems. Figure (9) shows plots of $|P(\phi)|^2$ and $|P_1(\phi)|^2$ versus ϕ with μ_m/μ_o appropriately adjusted so that the first zeros of $P(\phi)$ and $P_1(\phi)$ coincide for finite $\phi > 0$. The extent to which the continuum model can be approximated by a two-level system, parameterized with μ_o, in the domain $0 \leq \phi \leq 4.48$ is indicated by the similarity of the two curves. In this region effects will occur that have a qualitative similarity to self-induced transparency.[3] Considerably greater deviations begin to appear for larger ϕ as a consequence of the coherent dephasing of the ensemble of dipoles. Indeed, in the limit of high excitation the polarization is arbitrarily small since $\lim_{\phi \to \infty} P(\phi) = 0$. This statement is not true for the nondegenerate system and it constitutes an essential distinction between degenerate and non-degenerate media as we have represented them. A direct implication of this

result is that for high excitations (cf. Fig. (9)) degenerate systems tend to reradiate very little as compared to the comparable nondegenerate case. Finally, we point out that energy loss is associated with this behavior. Again, following Ref. (1) we calculate the energy loss per unit volume $W(\phi)$ as

$$W(\phi) = \frac{N\frac{\hbar\omega}{2}\int n(\mu)\,[\,1-\cos(\phi\mu)\,]\,d\mu}{\int n(\mu)\,d\mu} \tag{5}$$

giving

$$W(\phi) = \frac{N\hbar\omega}{2}\left[\,1-\frac{1}{\phi\mu_m}\sin(\phi\mu_m)\right] \tag{6}$$

Hence, at high excitations one approaches a constant loss given by

$$\lim_{\phi\to\infty} W(\phi) = \frac{N\hbar\omega}{2} \tag{7}$$

This loss, coupled with the fact that the degenerate system is qualitatively similar to the non-degenerate case only in the relatively low excitation range (cf. Fig. (9)), restricts the sample thickness for observation of reradiation effects. A sample that is too thin will not absorb and, hence, not reemit. On the other hand, an overly thick sample will present an overwhelming amount of loss, hence, leading to a diminished effect. The maximum observable effect will correspond to an intermediate sample thickness. On this basis the model predicts that coherent reradiation (pulse reshaping) should occur most dramatically at low pressure ($\tau << T_2$) and in a narrow range of input intensity for a sample corresponding to a few absorption lengths.[12] Our attitude is supported by both pulse propagation experiments in SF_6 and more detailed computer calculations[2] discussed below.

The experimental behavior, as described in section III B of this article, is substantially in agreement with this simple interpretation. The sample corresponded to nearly two absorption lengths. Examination of Figs. (5), (6), and (7) shows that a significant coherent reradiation effect was observed mainly in the region corresponding to the nonlinear transition region of the saturation curve in Fig. (7). Very little, if any effect, was observed for input intensities above or below this range.

More elaborate computer calculations[2] produced a very similar result. These computations incorporated the complications of a finite inhomogeneous width, a finite homogeneous width T_2^{-1}, and consequently, rendered a reasonable simulation of the SF_6 experiment. The continuous dipole moment distribution $n(\mu)$, discussed above, was approximated by a uniform distribution of discrete values spaced at equal intervals in μ. Equivalently, the calculations thus performed corresponded to a Q(10) transition of a symmetric top with the k-degeneracy removed. The saturation curve, the dependence of the pulse delay on input power, and the broadening of the pulse by reradiation are all very similar to our experimental results. This pulse broadening effect, as in the experiment, disappeared for input conditions corresponding to points either above or below the nonlinear transition region on the saturation curve. It should be noted

that the critical input condition for a non-degenerate two-level system would be $\theta_{in} = \pi$. The computer result for Q(10) indicated a critical situation for $\theta_{in} \cong 1.4\pi$.[14] Recall that for low excitations we argued that the continuum model could be approximated by a nondegenerate system with an appropriately chosen μ_o (cf. Fig. (9)). A value of $\mu_m/\mu_o = 1.43$ was calculated in that example. We believe that this compares favorably with the factor of 1.4 suggested by the computer results. Of course, such quantitative agreement is completely unexpected in view of the crude estimates that have been made. However, it does inspire respect for the continuum model approximation.

It is worth noting here that in the continuum limit one can easily estimate the dipole moment distributions corresponding to P, Q, or R-branch transitions of a symmetric top. We treat separately the cases distinguished by the presence or absence of k-degeneracy and include the effect of inhomogeneous broadening. The quantity $n(\mu, \omega)$ is defined as a density in μ - ω space such that $n(\mu, \omega)\, d\mu\, d\omega$ equals the number of radiators possessing dipoles moments between μ and $\mu + d\mu$ with resonant frequencies in an interval between ω and $\omega + d\omega$. The distribution in ω is assumed flat. This is a good approximation when the ratio of the saturation width $\Delta\omega_s = \mu\, \mathcal{E}/\hbar$ to the inhomogeneous width is less than unity. Hence, it is valid to put $n(\mu, \omega) = n(\mu)\, \rho(\omega) \propto n(\mu)$. Since $\rho(\omega)$ is a constant, we can integrate over a finite width $\Delta\omega$ giving

$$\int_{\Delta\omega} (n(\mu)\, \rho(\omega)\, d\mu)\, d\omega = n(\mu)\, \rho(\omega)\, \Delta\omega\, d\mu \equiv n'(\mu)\, d\mu \qquad (8)$$

Now, if the width $\Delta\omega$ is identified as the saturation width, then $n'(\mu) = c\mu\, n(\mu)$

since the saturation width is proportional to the dipole moment μ. The number c denotes an appropriate proportionality constant which does not concern us here. Hence, the inclusion of inhomogeneous broadening simply multiplies the dipole moment distribution $n(\mu)$ by μ. It remains to calculate $n(\mu)$ for the specific cases. This is accomplished by letting the projection quantum numbers m and k in the matrix elements[15] $\mu_j(m, k)$ represent continuous parameters in the interval $[-j, j]$ and assuming that each value of m or k is equally probable. Only transitions associated with light polarized along the z-direction are considered. The results for the Q-branches are quoted below. The quantity μ_m denotes the maximum dipole moment of the distributions so the results are valid only in the domain $0 \leq \mu \leq \mu_m$.

1. Q-branch, k-degeneracy removed; $n'(\mu) \propto \mu$.
2. Q-branch, k-degeneracy unbroken; $n'(\mu) \propto \mu(\mu_m - \mu)$.

Similar results can be obtained for the P and R-branches although they are somewhat tedious. These distributions show a tendency to peak more nearly about the maximum dipole moment μ_m of the distribution than the Q-branch results.

This section is concluded with some remarks on the intensity dependence of the photon echo.[5, 6] These considerations will affect the results of photon echo experiments in that they will lead to a substantial reduction in the echo intensity as a function of the input intensities. Ordinarily, for a nondegenerate system and a thin sample the echo intensity will be periodic in the input intensities. However, in the continuum model, the echo intensity will be strongly damped at high input intensities since $\lim_{\phi \to \infty} P(\phi) = 0$. Indeed, results consistent with this picture have been reported experimentally.[5] In this work[5]

the echo vanished completely and did not reappear at higher input intensities.

Recapitulating, we have introduced a crude, but we believe descriptive model for some coherent excitation processes in SF_6. We find that for low excitation the behavior of the degenerate system qualitatively resembles that of the simple, non-degenerate, two level system (cf. Fig. (9)). The predictions on pulse reshaping and absorption agree well with both our experimental findings and more sophisticated computer calculations.[2] And finally, it is shown that the anomalous intensity dependence of the photon echo in SF_6 can be understood as arising from the effects of degeneracy.

B. Calculations Corresponding to the Conditions of Section III C

The considerations described here pertain to the experimental results of section IIIC. The entire discussion assumes that no relaxation processes are operative. The principal effect reported in section IIIC was a considerable sharpening of the leading edge of the pulse under conditions of both high input intensity and an extremely thick sample (~20 absorption lengths). Figure (8), which illustrates this effect, shows that the decrease in the rise time is directly attributable to the energy removed from the leading edge of the pulse. The entire pulse, however, experiences a modest absorption of less than 20% of the total energy and the tail of the pulse is transmitted with no discernible effect. This behavior is typical of a saturation process; the ultimate rise time being determined by the time interval necessary, at that intensity, to saturate the medium. Because of the degeneracy of the SF_6 transition, this saturation behavior will occur even in the limit of a completely coherent excitation. We will call this an "effective" saturation process. It arises because the distribution of dipoles associated with the degeneracy cancel one another at high excitation levels and put the system into a state of essentially zero macroscopic polarization. However, a finite and constant

energy is absorbed in this process. Hence, in this context the term "saturation" describes a situation in which an additional increment of excitation does not change the macroscopic state of the medium, either its polarization or energy content. Naturally, the constant absorption, for a fixed sample, is relatively less and less as the input intensity and energy are increased. Indeed, in the continuum model presented in the preceding section, the macroscopic dipole moment left in the medium after the passage of the pulse is given by Eq. (3). This is a damped oscillating function which decreases rapidly as the pulse angle Θ is increased. At the same time the energy loss per unit volume tends to $\frac{N\hbar\omega}{2}$ as expression (7) indicates. In order to establish the credibility of this reasoning, we present the following argument. Consider only the leading edge of a pulse whose intensity I(t) is rising linearly as given by

$$I(t) \cong I_o \frac{t}{T_r} , \quad 0 \leq t \leq T_r \tag{9}$$

The quantity T_r is defined as the pulse rise time. We assume that the medium is saturated by this leading edge so that

$$\frac{\mu_m}{\hbar} \int_o^{T_r} E(t)\, dt = \frac{\mu_m}{\hbar} \int_o^{T_r} \sqrt{\frac{8\pi}{c} I(t)}\; dt = \Theta_m >> 1 \tag{10}$$

is valid for the characteristic value of the dipole moments associated with the transition. Since I_o and T_r are known from the experiment, one can calculate a rough estimate for the matrix element μ_m appearing in expression (10). With $I_o \cong 1\,kw/cm^2$, $T_r = 30\,nsec$, and assuming $\Theta_m \cong 20$, a simple computation gives $\mu_m \cong 3 \times 10^{-19}$ esu. This value is in good agreement[16] with estimates given for the relevant matrix elements in SF_6. The argument, of course, is only approximate, but since no adjustable parameters are at

our disposal, the agreement is significant.

The reasoning and conclusions of the preceding paragraph have been fully substantiated by computer calculations.[2] These calculations take into consideration, level degeneracy, inhomogeneous broadening and propagation effects arising from an optically thick sample. The radiation field is represented as plane, linearly polarized running wave.[17] Specifically, the computations were performed for a Q-branch transition corresponding to an angular momentum quantum number j = 10, Q(10). This particular choice was made becuase the matrix element distribution for Q(10) provides a discrete approximation to a continuous distribution of matrix elements used for discussion in the preceding section IVA. So we are motivated in our selection of a compatible case for discussion here. These calculations, with the parameters appropriately adjusted to correspond to the experimental situation, showed a pulse steepening effect remarkably similar to the one observed. This result is not peculiar to a Q(10) transition. The identical computations were performed for a P-branch transition with angular momentum quantum number j = 21, P(21). The conclusion was identical. Thus, as suggested in the remarks leading to Eq. (10), it appears that this pulse steepening effect emerges as a general phenomenon associated with the response of highly degenerate media to very intense, coherent pulses. In principle, the minimum rise time of this sharpening effect is limited by the effective saturation linewidth of the system. This quantity, from expressions (9) and (10) is given approximately by

$$T_r \cong \frac{3\Theta_m \hbar}{2\mu_m} \left(\frac{c}{8\pi I_o}\right)^{1/2} \qquad (11)$$

This time T_r can be made arbitrarily small by increasing the intensity I_o.

V. Discussions and Conclusions

Some of the complications of pulse propagation through an absorbing medium which arise from spatial degeneracy and overlapping levels have been examined both experimentally and theoretically. It is found that the effect of self-induced transparency, first described by Hahn, [3] is modified in an essential way. These modifications tend to reduce certain features associated with the effect. As is now well known, the strict case of self-induced transparency is only possible under very special circumstances. These conditions are described in Ref. (1). Unfortunately, these modifications tend to destroy many of the features of the pure effect, namely, a finite energy loss is assoicated with the pulse propagation, delay times are reduced, and the phenomenon of pulse break-up is suppressed. One of the most disappointing features of this result is that all these tendencies qualitatively modify the pulse propagation behavior in the same way as the introduction of a finite T_2. This will inevitably complicate the extraction of information relating to collisions when, in future experiments, one operates in a regime where T_2 is comparable to the pulse width.

Our analysis is based on a degenerate, homogeneously broadened model. This is done in order to point out the differences between degenerate and non-degenerate systems. Inhomogeneous broadening which is present in our experiments apparently modifies both cases similarly.

Any study of this nature using SF_6 involves obvious difficulties. It has been stressed that the detailed behavior of pulse propagation depends crucially on quantum numbers of the absorbing states. However, the precise level

structure of SF_6 is both complicated and unknown. In our analysis we have attempted to utilize the apparently continuous absorption through the introduction of a continuum model (a continuum in ω and μ). This program views the spectral complications in such a way that a simplification obtains. On this basis a number of statements concerning the behavior of coherent optical excitations were made. All these considerations were in the limiting case of $T_2 \rightarrow \infty$. Thus, the main thrust of this research has been focused on the examination of degeneracy effects in a continuum limit. Basically, two different effects were observed and described on the basis of the continuum model. The first involved high excitation of a very thick sample. In this case an effective saturation behavior was observed which led to a sharpening of the leading edge of the input pulse. This is a fully coherent effect and a general feature of degenerate systems under a broad range of circumstances. The second effect illustrated pulse reshaping and reradiation phenomena as they occur in degenerate media. It was shown that under suitable conditions (moderate excitation and a sample around one absorption length) the results could be qualitatively understood by an equivalent two-level system. A finite loss is assoicated with propagation under all these conditions so no strict transparency is observed.

VI. Acknowledgments

We are indebted to Professor A. Javan for his continued support, encouragement, and advice through the entire course of this work. We also gratefully acknowledge Dr. F. A. Hopf and Professor M. O. Scully for assistance and collaboration on the computer analysis. We cordially express our thanks to Mr. P. Hoff and Professor H. Haus for the loan of the detector used in this experiment.

VII Supplement

A - Unusual Experimental Observation in SF_6

An unusual experimental result was obtained in a pressure and intensity region well above that described in IIIB. This result is highly suggestive of a self focussing effect. The SF_6 pressure in the 3.4 meter cell was around 50 mTorr and the input intensities were approximately 10^3 times above the intensity for maximum pulse reshaping as discussed in Section IIIB. Figure (10) illustrates one such result. The input pulse is essentially the same as shown in Fig. (2). The pulse appears to have broken up into two well resolved pulses with a node very nearly occuring between them. This pulse configuration, the sharper one travelling faster and both of nearly similar areas, is precisely the wave form to which a 4π input pulse is expected to evolve for a non-degenerate system as discussed by Hahn.[3] However, this is not happening here, at the very least, in view of the effects of degeneracy. Indeed, careful examination indicates that the two peaks are not passing through the same volumes in the absorption cell. The intensity ratio can be reversed by manipulating irises. A complicated phenomenon appears to be taking place. Experimentally, the situation is ripe for violations of an infinite plane wave description. The sample has an optical depth more than 20 absorption lengths and our input mode pattern is essentially diffraction limited. The plane wave model[17] is very probably useless for such circumstances (i.e. diffracting input and sample absorption lengths >> 1).

B - CO_2 Fluorescence Calculations

It was stated in the preceding sections of this article that the unknown spectroscopic properties of SF_6 considerably complicated the analysis of coherent pulse transmission experiments. On the other hand, CO_2, even though it possesses the advantage of a known structure, is practically useless in propagation experiments because its absorption is too small. In this appendix we present the results of calculations pertaining to CO_2 in an experimental situation where the known spectroscopic information is used to advantage. It is a variant of the transient nutation effect well known in NMR. The experiment is sensitive to any irreversible dephasing time T_2, but does not operate on a propagation effect. This provides a generous simplification in that only Schrodinger's equation is used in this treatment, Maxwell's equation being unnecessary since no propagation effects are considered (i.e. optically thin medium). CO_2 gas absorbs weakly at 10.6μ because the absorption occurs from an excited state $\sim 1300\,cm^{-1}$ above the ground state (see Fig. (11)). However, the 4.3μ transition $00^01 \rightleftharpoons 00^00$ is infrared active and the spontaneous radiation radiated subsequent to excitation at 10.6μ is readily detectable.[18] For a fully coherent excitation from $10^00 \rightarrow 00^01$ the intensity of the spontaneous emission from the 00^01 state is proportional to the sum of the upper state populations. We denote the upper state amplitudes by $a_{m(.)}$ and consider excitation on only one of the vibrational-rotational transitions in the 10.6μ band. The spontaneous emission intensity has been calculated as a function of input intensity for a linearly polarized square wave input pulse of height $\mathcal{E}_0$ and width τ. The effect of inhomogeneous broadening is included. If the upper state amplitudes are assumed to be zero before the pulse, a standard solution of the two-level problem, ignoring anti-

resonant terms, gives the upper state populations $|a_m(\Delta\omega, \mathcal{E}_o, \tau)|^2$ as

$$|a_m(\Delta\omega, \mathcal{E}_o, \tau)|^2 = \frac{(\mu_m \mathcal{E}_o)^2}{(\omega - \omega')^2 + (\mu_m \mathcal{E}_o)^2} \sin^2 \left\{ \tau \left[(\omega - \omega')^2 + (\mu_m \mathcal{E}_o) \right]^{1/2} \right\} \quad (12)$$

where $\Delta\omega = \omega - \omega'$

$\mu_m = \langle \text{upper, m} | \vec{\mu}_{op} | \text{lower, m} \rangle$, $\hbar = 1$

(diagonal in m since input is linearly polarized along the z-direction)

ω = angular frequency of optical radiation

ω' = angular center frequency of irradiated system.

If the inhomogeneously broadened resonance has a center at ω_o and is described by a gaussian distribution of width $\Delta\omega_D$, then the 4.3μ spontaneous emission signal is proportional to

$$I(\omega, \mathcal{E}_o) = \int_0^\infty d\omega' e^{-\frac{(\omega' - \omega_o)^2}{\Delta\omega_D}} \sum_{m=-j}^{j} (\mu_m \mathcal{E}_o)^2 \frac{\sin^2 \left\{ \tau \left[(\omega - \omega)^2 + (\mu_m \mathcal{E}_o)^2 \right]^{1/2} \right\}}{(\omega - \omega')^2 + (\mu_m \mathcal{E}_o)^2} \quad (13)$$

The summation extends over the $2j+1$ degenerate levels associated with the molecular transition. Naturally, we have assumed that $\tau \ll T_2$ in these calculations. We have also ignored any dependence on the input pulse shape as this is known to be weak (square, gaussian or hyperbolic secant wave forms probably result in a 5% deviation or less).

Figure (12) illustrates the results for two cases of interest. A curve corresponding to the opposite case $T_2 \ll \tau$, calculated by the normal steady state saturation formula, is included for comparison. The modulation of the output intensity arises from the coherent excitation of states with differing dipole moments.

Experimentally, one measures the 4.3μ spontaneous emission intensity versus input intensity parametrically as a function of CO_2 pressure. In this way, T_2 can be roughly defined by the pressure at which the intensity modulation becomes smeared. At this pressure $T_2 \sim \tau$. An experiment of this type is presently under way in our laboratory.

C: Remarks Concerning Photon Echo Polarization for an Optically Thick Medium

Gordon et al.[6] have calculated the photon echo polarization dependence on the relative polarization of the excitation pulses for P, Q, and R-branch transitions for several values of angular momentum j. They give the relative echo polarization under the following conditions;

a) the echo intensity is at a maximum and

b) the sample is optically thin.

These results have a dependence on the excitation pulse intensities and will, therefore, not apply to an optically thick medium. Indeed, their experiment, which was conducted on an optically thick sample, led them to conclusions that they themselves described as difficult to believe (to wit $j = 0 \rightleftharpoons j' = 1$ or $j = 1 \rightleftharpoons j' = 1$ transition).

A complete solution of the echo polarization problem involving propagation effects necessitates an elaborate computer analysis which is not presented here. Instead, we indicate how the qualitative effect of a thick sample can be understood in considerably simpler terms as derived from the calculation valid for a thin sample. At this point we follow the work of Gordon et al.[6] in defining a vector $\vec{Q}$[19] which describes the echo polarization vector by

$\epsilon_{echo} = \frac{\vec{Q}}{|\vec{Q}|}$ and the echo intensity by a quantity proportional to $|\vec{Q}|^2$. Consider the geometry illustrated in Fig. (13). Then $\vec{Q}$ is given[6] by

$$\vec{Q} = \sum_{m, m', m''} \sin\left(\frac{\phi_{2m}}{2}\right) \sin\left(\frac{\phi_{2m'}}{2}\right) \sin\left(\phi_{1m''}\right) .$$

$$\langle a, m | \vec{P}_{op} | b, m' \rangle \langle a, m' | e^{-i\psi J_y} | a, m'' \rangle \langle b, m'' | e^{i\psi J_y} | b, m \rangle \qquad (14)$$

where

$$\phi_{1i} \equiv 2 \langle a, i | P_z | b, i \rangle \int_{\text{first pulse}} F_{1(t)}\, dt$$

$$\phi_{2i} \equiv 2 \langle b, i | P_z | a, i \rangle \int_{\text{second pulse}} F_{2(t)}\, dt$$

$F_{i(t)}$ = envelope of excitation pulse, $i = 1, 2$

$\vec{P}_{op} \equiv$ dipole moment operator

$\langle a, i |$ = lower state a, i^{th} sublevel

$\langle b, i |$ = upper state b, i^{th} sublevel

J_y = y - component of angular momentum operator.

The triple summation is taken over all the degenerate sublevels. In a thick sample the excitation functions ϕ_{2i} and ϕ_{1i} vary considerably through the sample. Thus, for $m \neq m'$ the factor $\sin\left(\frac{\phi_{2m}}{2}\right) \sin\left(\frac{\phi_{2m'}}{2}\right)$ appearing in Eq. (14) will tend to a small quantity due to the effective averaging over a range of ϕ_{2m} and $\phi_{2m'}$. However, for $m = m'$ the $\sin^2\left(\frac{\phi_{2m}}{2}\right)$ will tend toward a value of 1/2. This averaging process then causes the summation to be dominated by the terms for which $m = m'$. The vector property of $\vec{Q}$ is contained in the matrix element $\langle a, m | \vec{P}_{op} | b, m' \rangle$ which for $m = m'$ goes over to $\langle a, m | P_z | b, m \rangle$, P_x and P_y vanishing. Hence, $\vec{Q}$ lies along the polarization of the second pulse $\epsilon_2 = 1_z$ independent of the angular momentum

quantum states of the participating levels. Of course this argument is incomplete in that it ignores any propagation effects. In spite of this, however, it fairly clearly establishes the tendency of thick samples with degenerate levels to produce echo polarizations which lie along the second pulse polarization. However, this simple theory does not give a $\cos^2\psi$ dependence for the echo intensity. This intensity behavior is, in general, quite complicated.

REFERENCES

1. C.K. Rhodes, A. Szöke, and A. Javan, Phys. Rev. Letters 21, 1151 (1968).
2. These computer calculations have been performed in collaboration with Dr. F.A. Hopf and Professor M. O. Scully. The details of these calculations, along with a number of other results, will appear in a future publication.
3. S. L. McCall and E. L. Hahn, Phys. Rev. Letters 18, 908 (1967).
4. C.K.N. Patel and R. E. Slusher, Phys. Rev. Letters 19, 1019 (1967).
5. C.K.N. Patel and R. E. Slusher, Phys. Rev. Letters 20, 1087 (1968).
6. J. P. Gordon, C.H. Wang, C.K.N. Patel, R.E. Slusher, and W.J. Tomlinson, Phys. Rev. to be published.
7. This result was reported to us by Mr. P. Hoff and Professor H. Haus, from whom the detector was borrowed. Also see T. Bridges, H. Haus, and P. Hoff, Applied Physics Letters 13, 316 (1968).
8. H. Brunet, Compt. Rend. 264, 1721.(1967).
9. T.K. McCubbin, Jr., Air Force Cambridge Research Laboratories Report AFCRL-67-0437, (1967).
10. F. A. Hopf and M. O. Scully, to be published.
11. The "passing" of the input pulse can be distinguished only if $P(\phi)$ is small, otherwise appreciable ringing will occur and the pulse will appear to broaden. This weakness is inherent in any treatment that uses a homogeneously broadened model. Hence, we will regard expressions (2) through (7) as valid for ranges of ϕ where $P(\phi)$ is sufficiently small. These ranges will occur near the zeros of $P(\phi)$ and for ϕ large, since $|P(\phi)|$ decreases rapidly as ϕ increases (cf. Fig. (9).)

REFERENCES (cont.)

12. We appreciate that this point is not too precise. However, for samples of less than two absorption lengths and for input intensities in the region of the knee of the saturation curve (cf. Fig. (7)) the excitation throughout the sample is roughly uniform. We argue further, that in such low absorption samples, the reradiated energy can be considered, in a first approximation, as essentially unaffected by this absorption.

13. R.H. Dicke, Phys. Rev. 93, 99 (1954); N. Bloembergen and R.V. Pound, Phys. Rev. 95, 8 (1954); S. Bloom, J. Appl. Phys. 28, 800 (1957).

14. The angle Θ_{in} is calculated with respect to μ_m, which in this case is equal to unity.

15. C.H. Townes and A.L. Schawlow, "Microwave Spectroscopy", McGraw-Hill, New York, 1955, pg. 96.

16. From low level absorption experiments we estimate the value of the average matrix element associated with this absorption as $\sim 5 \times 10^{-19}$ esu. Professor J. Steinfeld, in an independent study, estimates a value of $\sim 3 \times 10^{-19}$ esu (private communication).

17. It is important to observe that this plane wave assumption automatically excludes from consideration all phenomena associated with the curvature of surfaces of constant phase. An important example is self-focusing.

18. L.O. Hocker, M.A. Kovacs, C.K. Rhodes, G.W. Flynn, and A. Javan, Phys. Rev. Letters 17, 233 (1966).

19. For a derivation of $\vec{Q}$, the interested reader should examine Ref. (6). They[6] calculate the response of the medium using standard density matrix methods and then isolate the term responsible for the echo. This, modulo a multiplicative factor, is $\vec{Q}$.

FIGURE CAPTIONS

1. Schematic Diagram of the Experimental Apparatus

   Key: A - wideband amplifier, rise time ~ 3 nsec;

   B - NaCl flat beam splitter, uncoated

   D_1, D_3 - Ge:Au liquid N_2 cooled detectors

   D_2 - Ge:Cu liquid He cooled detector

   G - grating

   I_1, I_2, I_3 - adjustable irises

   K - grating monochromator

   L_1, L_2 - BaF_2 lenses

   M_1 - $7\frac{1}{2}$ meter radius Ge mirror, uncoated

   M_5 - 8 meter mirror

   S_1 - attenuator cell, 15 cm long

   S_2 - 3.4 meter SF_6 absorption cell

   R - flat rotating Q-switch mirror

   T - 3 meter Brewster window laser tube

2. Typical Q-switched Laser Pulse. Horizontal Scale = 100 nsec/cm

3. Linear absorption data for the absorption of the P(16), P(18), and P(20) lines ($10^0 0 \rightleftharpoons 00^0 1$ band) of CO_2 in SF_6 for SF_6 pressures below 50 mTorr.

4. The SF_6 spectrum in the region of 10.6 μ as taken from Brunet.[8] The upper numbers are associated with points on the SF_6 spectrum. The relative positions of the P(16), P(18), and P(20) transitions of CO_2 are described by the lower arrows.

5. A sequence of output pulses at an SF_6 pressure of 6 mTorr, for varying input intensity of the CO_2 P(16) transition. In the sequence the input intensity

FIGURE CAPTIONS (cont)

5. (cont) rises monotonically from the top left to the lower right reading successively across the page. The time scale for all photographs is 100 nsec/cm.

6. A delay curve; the position of the output pulse maximum versus the input pulse intensity of the CO_2 P(16) line. The SF_6 pressure was 6 mTorr. The delay times are in units of the SF_6 inhomogeneous width, $T_2^* = 50$ nsec.

7. The saturation curve which corresponds to the data illustrated in Fig. (6); output pulse intensity versus input pulse intensity. The SF_6 pressure was 6 mTorr. The small peak on the input pulse has precursor type behavior as indicated by the linear plot that represents its response.

8. As output pulse sequence for the CO_2 P(16) line as the SF_6 pressure is slowly swept. The pulse steepening occurs at an SF_6 pressure corresponding approximately to 40 mTorr. Pulse intensity is plotted vertically while the time scale on the horizontal is 50 nsec/cm.

9. Plots of the polarization density functions squared, $|P(\phi)|^2$ and $|P_1(\phi)|^2$, for the continuum model and the quasi-equivalent two-level system, respectively, versus ϕ. The condition for the coincidence of the first zeros of $P(\phi)$ and $P_1(\phi)$ for finite $\phi > 0$ is $\mu_m/\mu_o = 1.43$.

10. A double peaked output pulse wave form from the 3.4 meter absorption cell. The SF_6 pressure was ~ 50 mTorr and the input pulse corresponded to that illustrated in Fig. (2). Pulse intensity is plotted vertically while the horizontal time scale corresponds to 50 ns/cm.

11. A partial CO_2 energy level diagram showing the vibrational states relevant to the 10.6μ absorption and the subsequent 4.3μ fluorescence.

FIGURE CAPTIONS (cont)

12. Intensity of spontaneous emission at 4.3μ versus intensity ($\mathcal{E}_o^2$) of the excitation pulse at 10.6μ. Two cases are shown; $j = 0 \rightarrow j' = 1$ and $j = 16 \rightarrow j' = 17$. The third smooth curve represents the result for a steady state situation, $T_2 \ll \tau$.

13. The geometry for the echo polarization;
$\hat{\epsilon}_1$ = polarization vector of the first pulse,
$\hat{\epsilon}_2 = 1_z$ = polarization vector of the second pulse,
both input pulses propagate along the y-axis with wave vectors $\vec{k}_1 = \vec{k}_2 = k\hat{1}_y$.

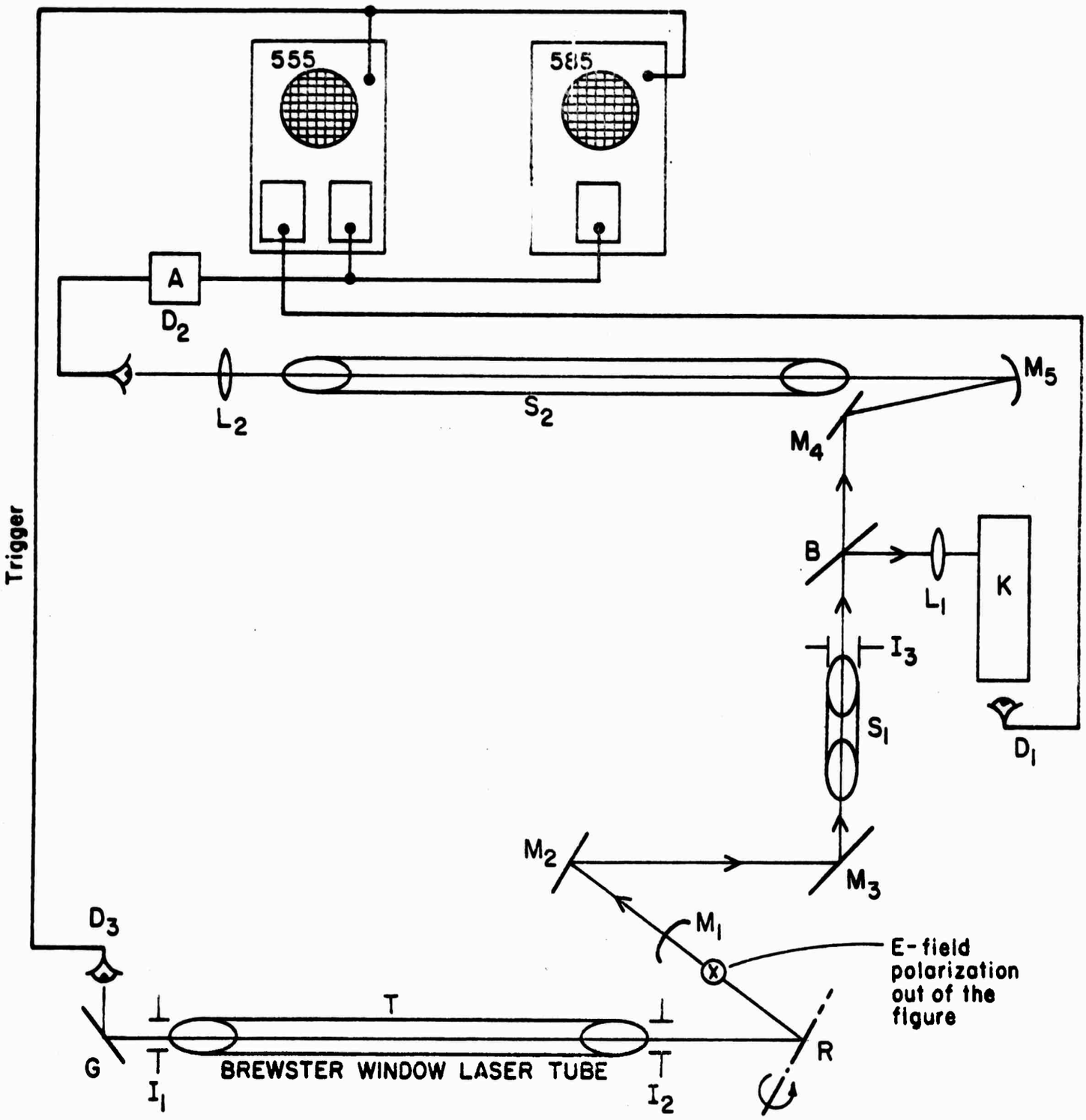
555
585
A
D2
L2
S2
M5
M4
B
L1
K
I3
S1
D1
M2
M3
M1
D3
E-field
polarization
out of the
figure
T
G
I1
BREWSTER WINDOW LASER TUBE
I2
R
Trigger

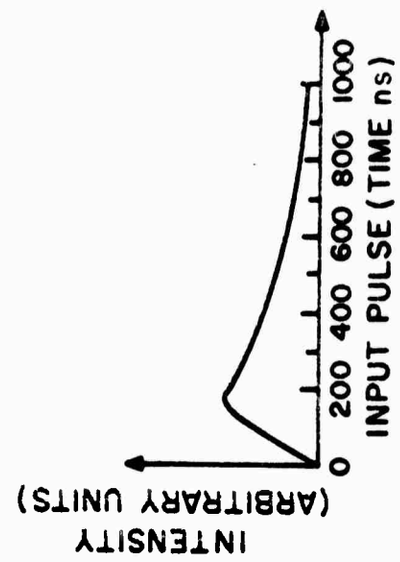
INTENSITY
(ARBITRARY UNITS)
0
200
400
600
800
1000
INPUT PULSE (TIME ns)

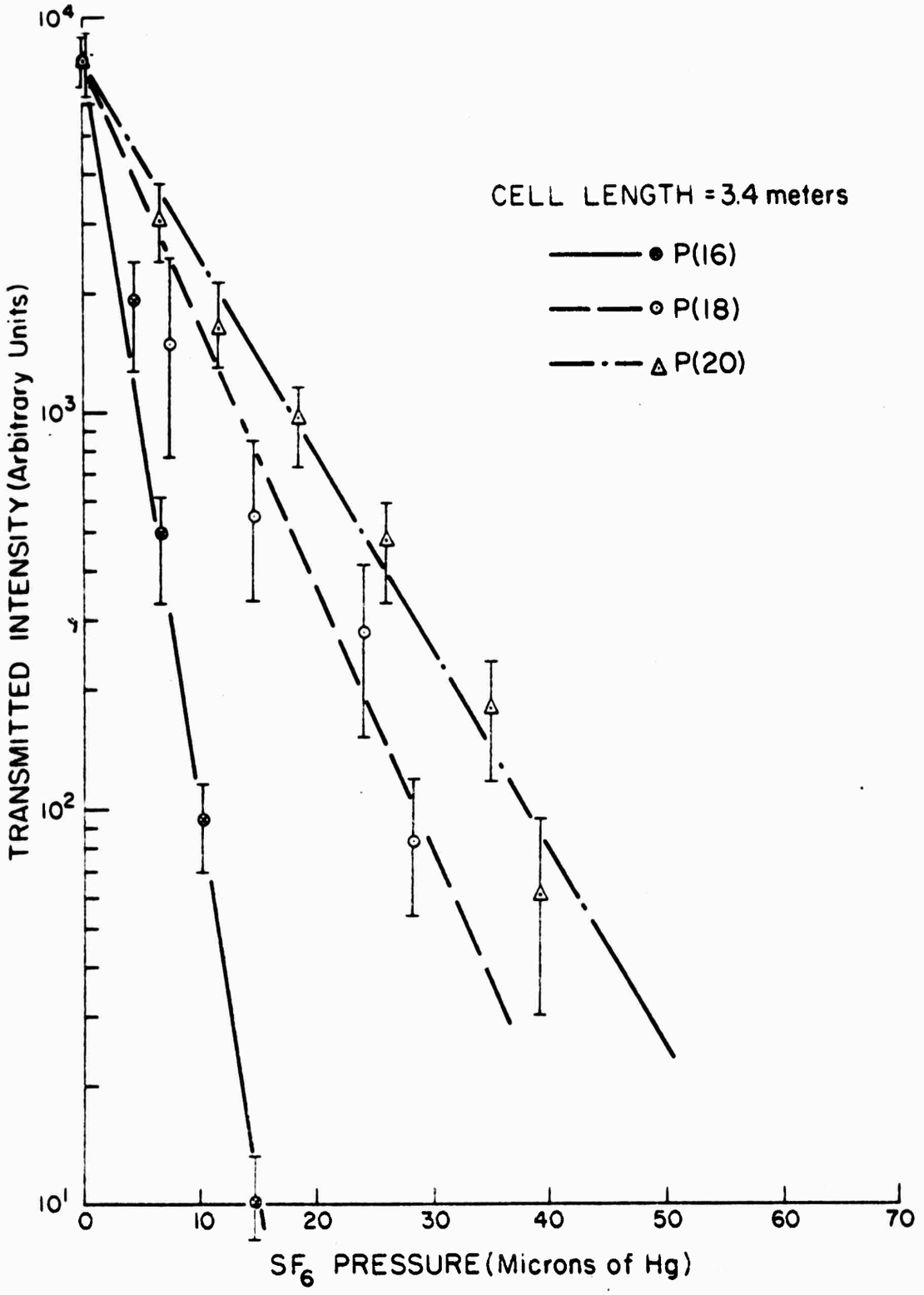
CELL LENGTH = 3.4 meters
P(16)
P(18)
P(20)
TRANSMITTED INTENSITY (Arbitrary Units)
10^4
10^3
10^2
10^1
0
10
20
30
40
50
60
70
SF_6 PRESSURE (Microns of Hg)

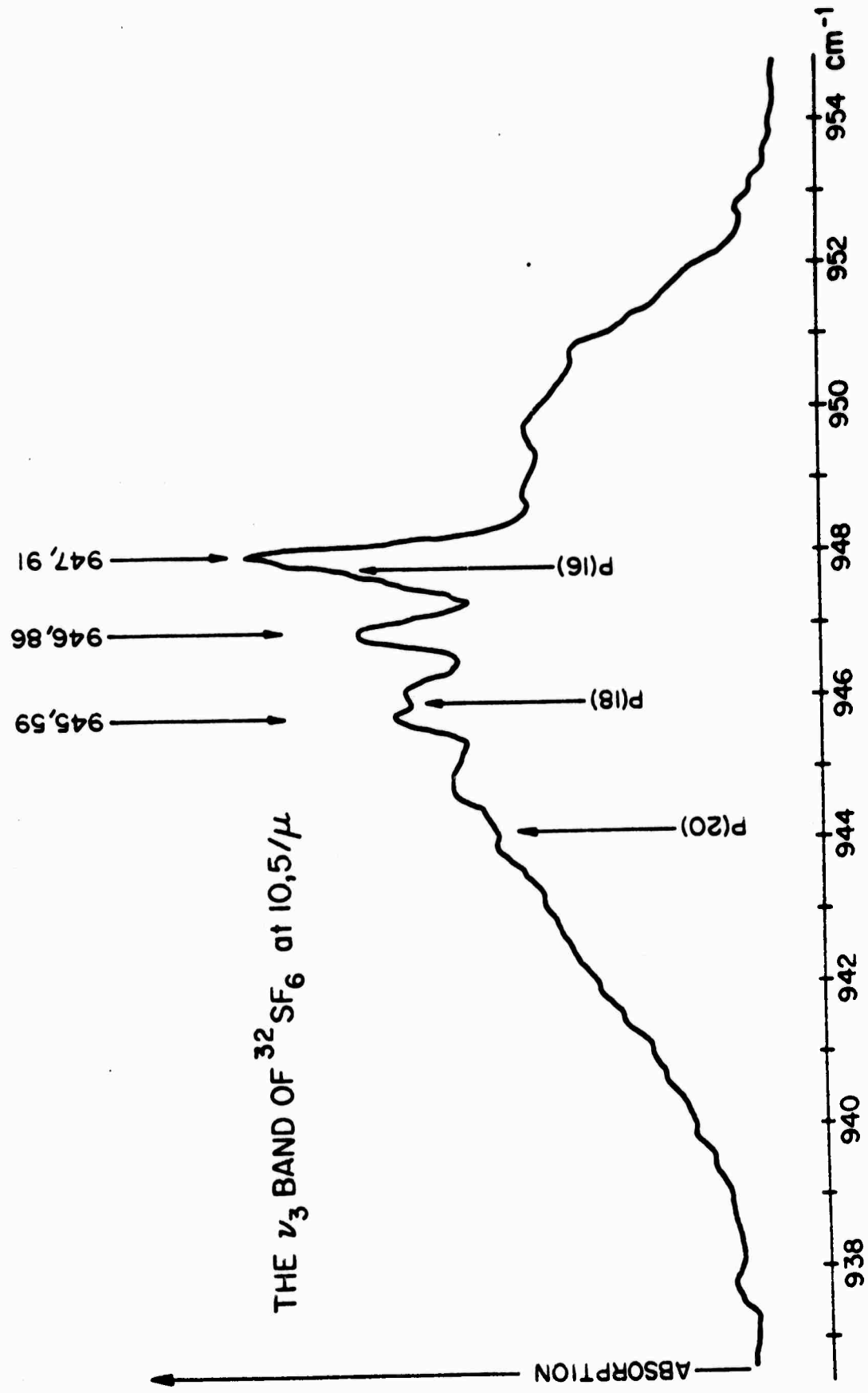
THE ν_3 BAND OF $^{32}SF_6$ at 10,5/μ
ABSORPTION
938
940
942
944
946
948
950
952
954 cm^{-1}
P(20)
P(18)
P(16)
945,59
946,86
947,91

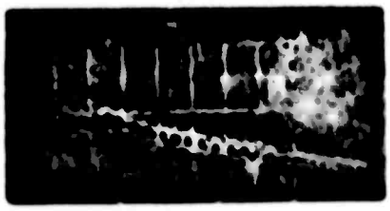

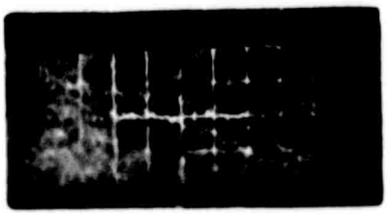

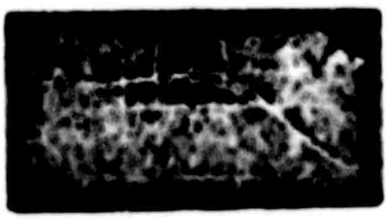

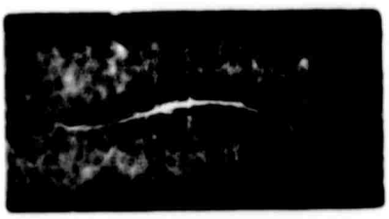

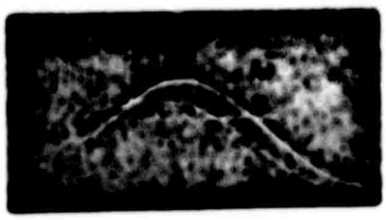

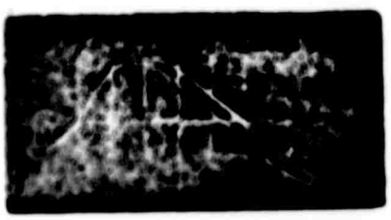

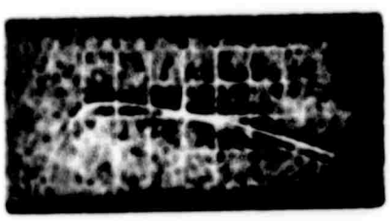

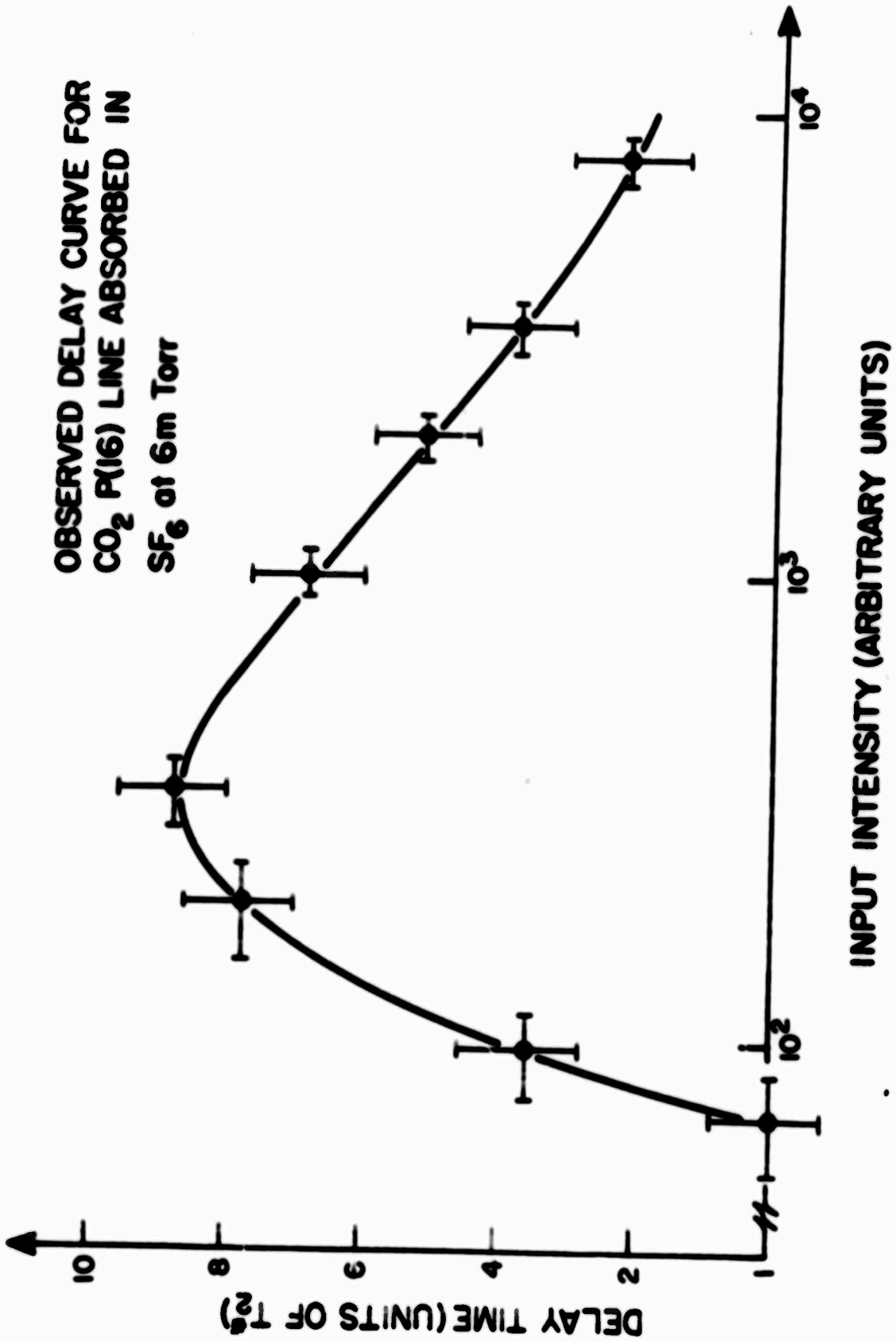
OBSERVED DELAY CURVE FOR
CO_2 P(16) LINE ABSORBED IN
SF_6 at 6m Torr
DELAY TIME (UNITS OF T_2^0)
INPUT INTENSITY (ARBITRARY UNITS)
1
2
4
6
8
10
10^2
10^3
10^4

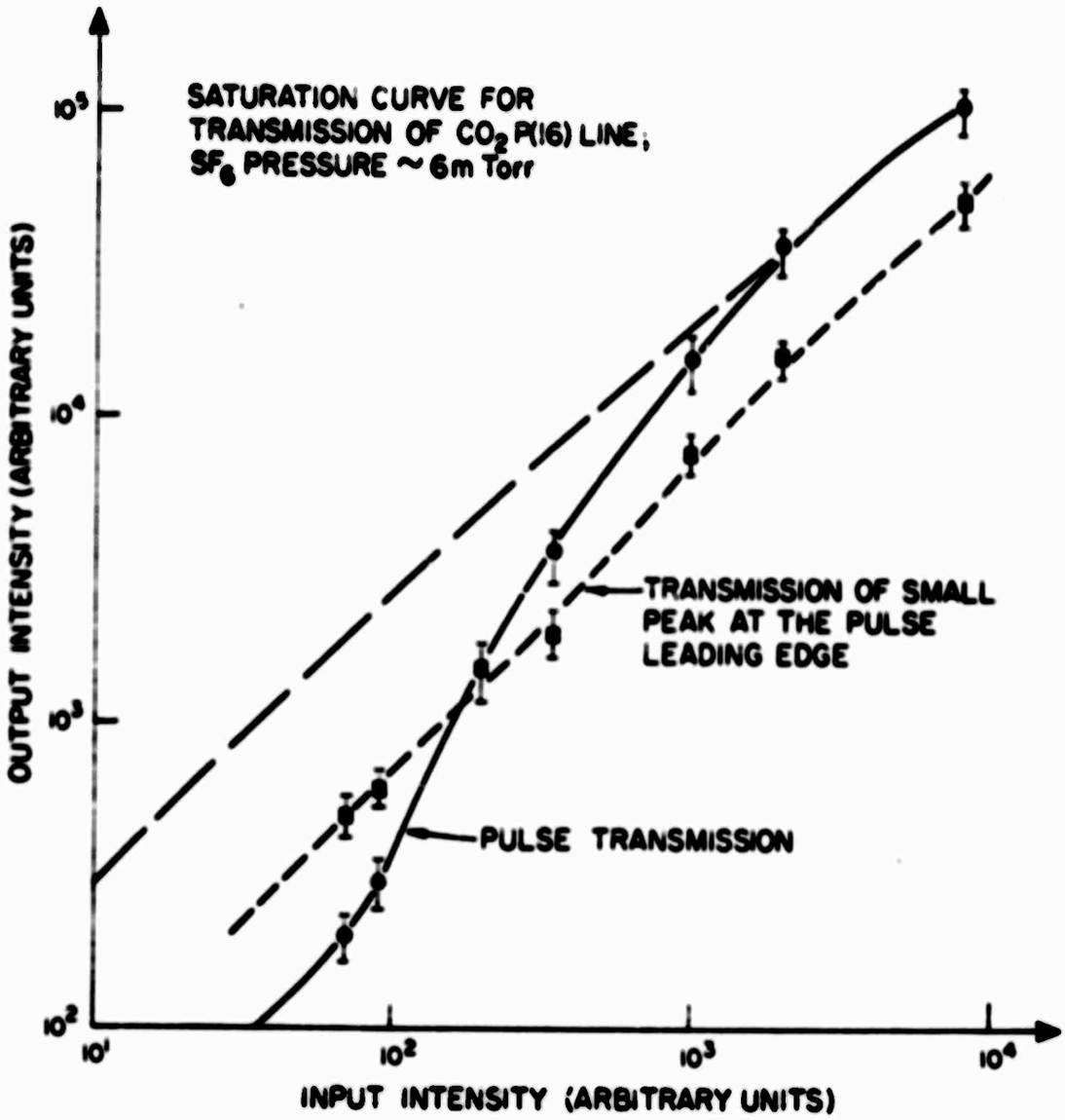
SATURATION CURVE FOR
TRANSMISSION OF CO_2 P(16) LINE;
SF_6 PRESSURE ~ 6m Torr
TRANSMISSION OF SMALL
PEAK AT THE PULSE
LEADING EDGE
PULSE TRANSMISSION
OUTPUT INTENSITY (ARBITRARY UNITS)
INPUT INTENSITY (ARBITRARY UNITS)
10^5
10^4
10^3
10^2
10^1
10^2
10^3
10^4

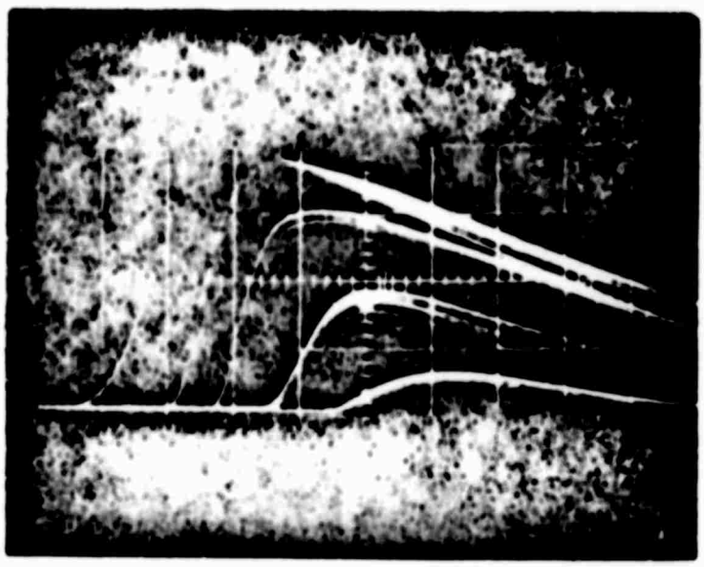

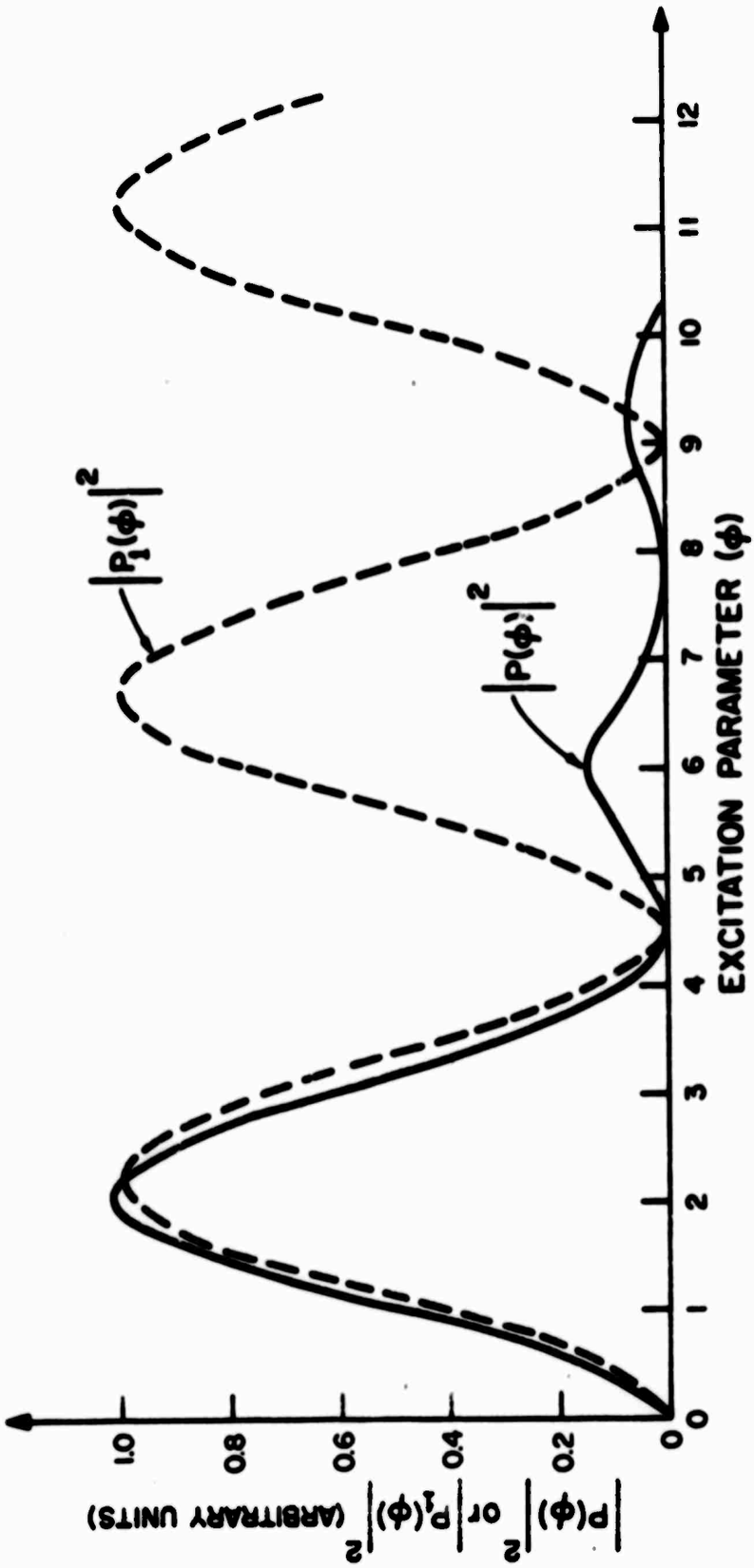
$|P(\phi)|^2$ or $|P_1(\phi)|^2$ (ARBITRARY UNITS)
0.0
0.2
0.4
0.6
0.8
1.0
0
1
2
3
4
5
6
7
8
9
10
11
12
EXCITATION PARAMETER (ϕ)
$|P_1(\phi)|^2$
$|P(\phi)|^2$

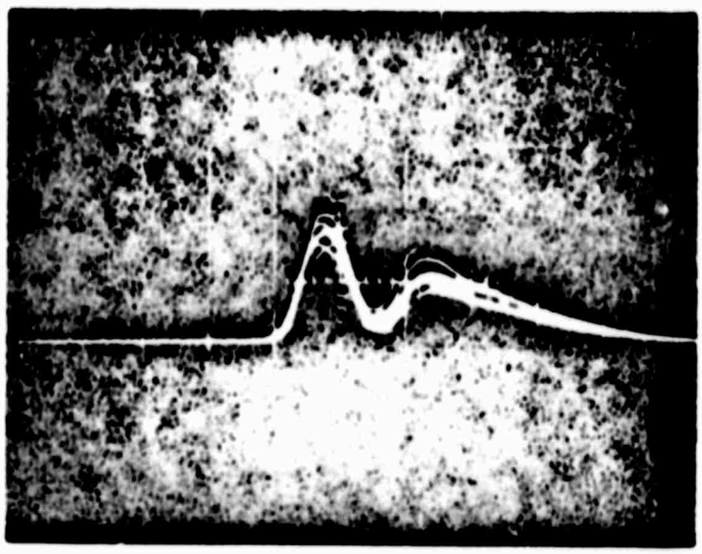

Partial CO_2 Level Diagram

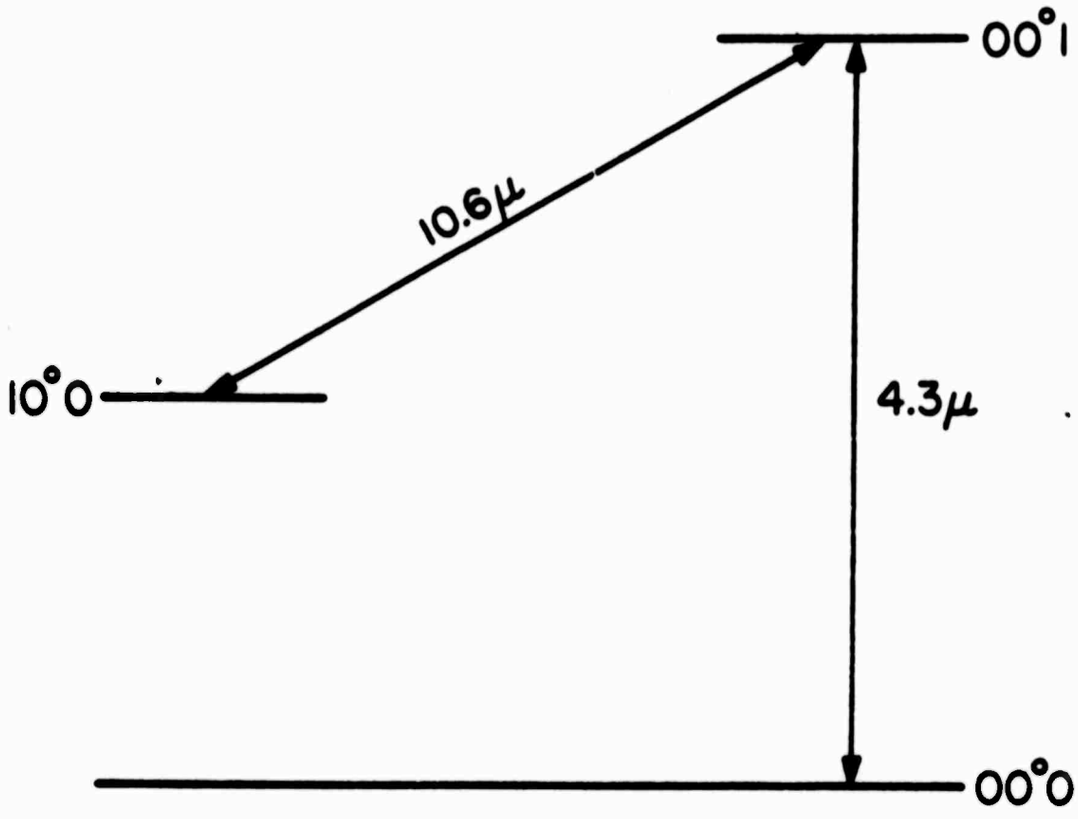

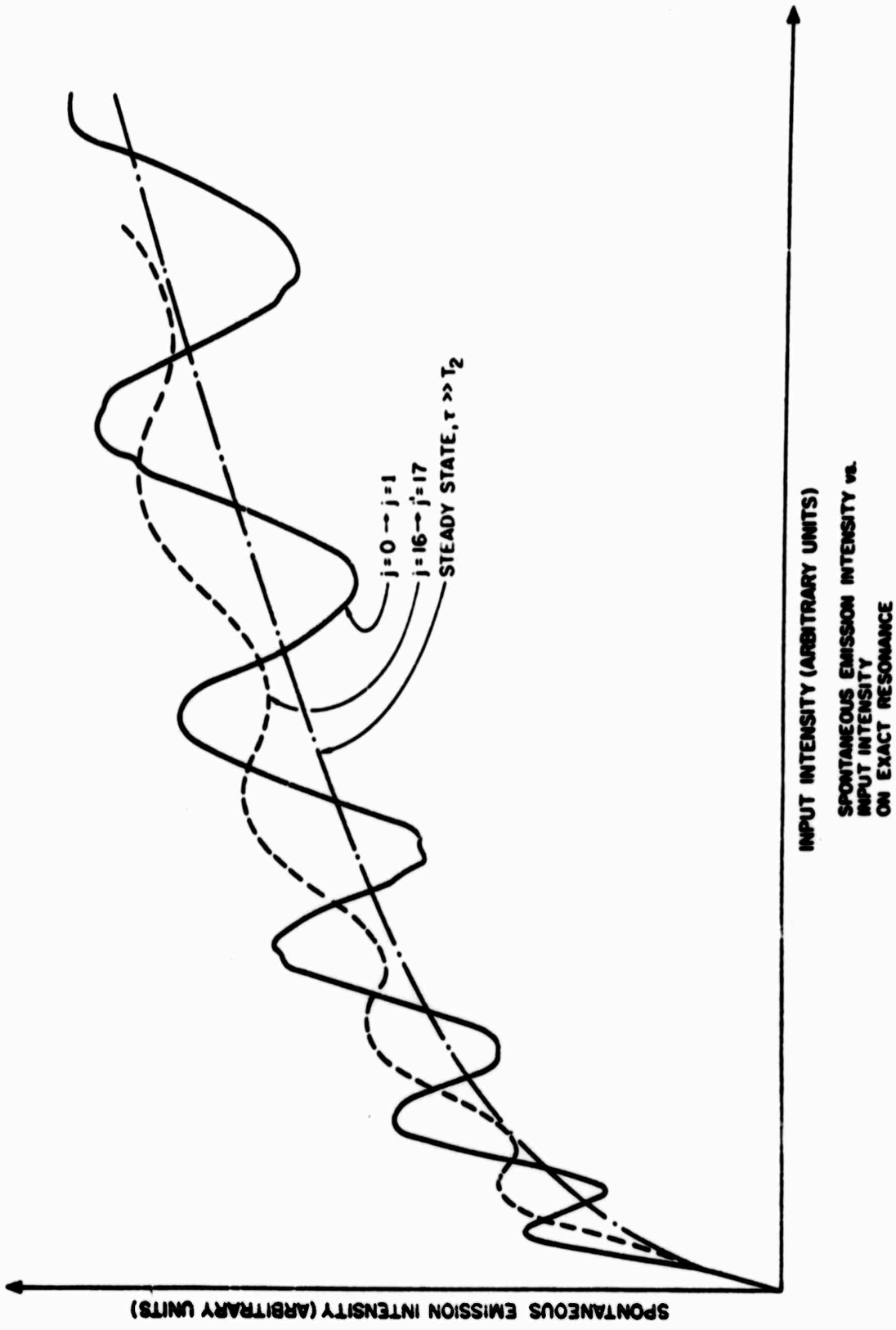
SPONTANEOUS EMISSION INTENSITY (ARBITRARY UNITS)
INPUT INTENSITY (ARBITRARY UNITS)
SPONTANEOUS EMISSION INTENSITY vs. INPUT INTENSITY ON EXACT RESONANCE
j = 0 → j = 1
j = 16 → j = 17
STEADY STATE, $\tau \gg T_2$

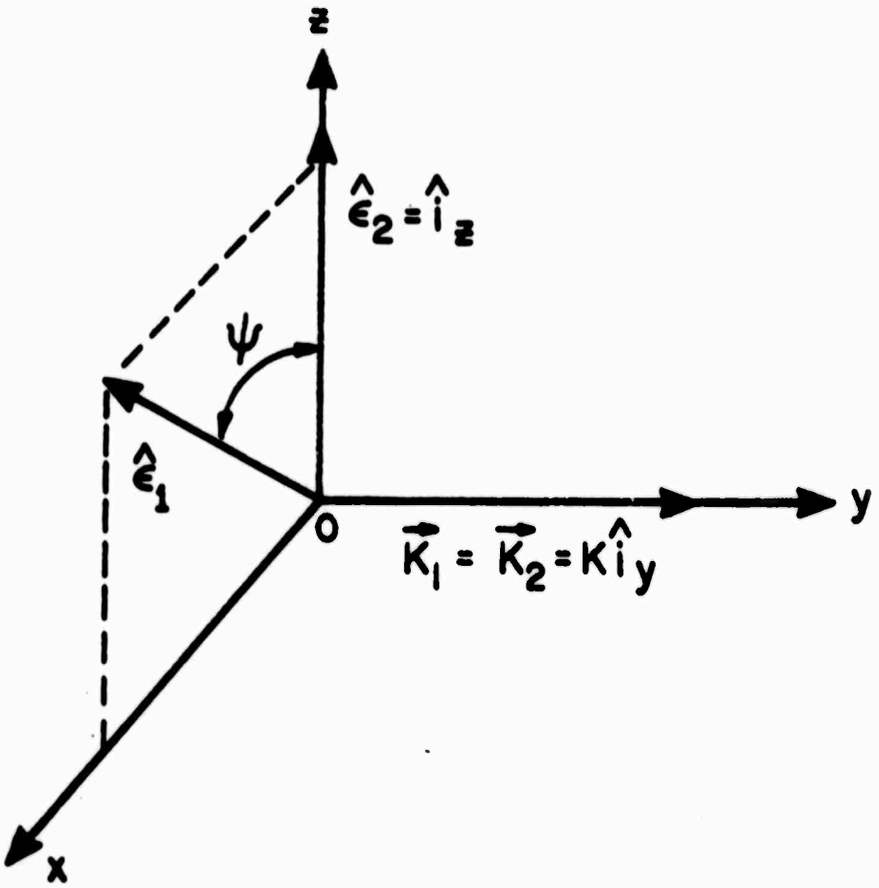

ECHO POLARIZATION GEOMETRY

Unclassified

Security Classification

DOCUMENT CONTROL DATA - R & D

(Security classification of title, body of abstract and indexing annotation must be entered when the overall report is classified)

1. ORIGINATING ACTIVITY (Corporate author)
Massachusetts Institute of Technology
Cambridge, Massachusetts 02139

2a. REPORT SECURITY CLASSIFICATION
Unclassified

2b. GROUP

3. REPORT TITLE
"Application of Gas Lasers to Studies of Fundamental Molecular and Atomic Processes"

4. DESCRIPTIVE NOTES (Type of report and inclusive dates)
Annual Technical Report # 2 1/1/69 through 12/31/69

5. AUTHOR(S) (First name, middle initial, last name)
Professor Ali Javan; Principal Investigator

6. REPORT DATE	7a. TOTAL NO. OF PAGES	7b. NO. OF REFS
April 10, 1970	66	26

8a. CONTRACT OR GRANT NO.	9a. ORIGINATOR'S REPORT NUMBER(S)
N00014-67-A-0204-0014 b. PROJECT NO. NR 015-717/5-7-68 Code 421 c. d. ARPA Order # 306	Annual Technical Report # 2 9b. OTHER REPORT NO(S) (Any other numbers that may be assigned this report)

10. DISTRIBUTION STATEMENT
Distribution of this document is unlimited

11. SUPPLEMENTARY NOTES	12. SPONSORING MILITARY ACTIVITY
	Office of Naval Research Advanced Research Projects Agency ARPA Order # 306

13. ABSTRACT

This report covers laser and quantum electronics research in several areas. A bi-stable optical element has been developed which can produce short pulses of variable length and intensity. A standing-wave saturation technique has been applied to the measurement of rotational relaxation linewidths in CO_2. Molecular relaxation processes are being studied using coherent optical processes. An experimental and theoretical study of short pulse propagation in SF_6 has been completed. Considerations are also given relating to propagation of zero-degree pulses. Plans are under way to study relaxation processes in the CO laser.

DD FORM 1 NOV 68 1473 (PAGE 1)

S/N 0101-807-6801

Unclassified

Security Classification

3ND PPSO 13152

KEY WORDS	LINK A		LINK B		LINK C	
	ROLE	WT	ROLE	WT	ROLE	WT
bi-stable optical element						
standing-wave saturation resonances						
relaxation processes						
short pulse transmission						